Numerical Computation of Phase from Amplitude at Optical Frequencies

By D. E. THOMAS

(Manuscript received January 31, 1963)

This paper presents phase tables for use in determining phase from amplitude or vice versa at optical and higher frequencies. The new tables, combined with tables previously published by the author, are believed to make possible the determination of phase from amplitude or vice versa of any minimum phase function occurring in any area of the physical sciences, and at any place in the frequency spectrum. The phase is determined by a summation process based on Bode's straight-line approximation method. The paper gives a brief historical background of the method, discusses the application of the numerical phase summation technique to optical and higher frequencies, describes the derivation of new tabulations useful at these frequencies, and gives quantitative examples of their use. A table expanding the existing tables of phase of a semi-infinite unit slope near f/f_0 equal to one is given. Additional tables of phase of a unit line segment and a new straight-line element, the unit wedge, are given. Finally, there is a brief discussion of the potential of the method in solving physical and engineering problems.

I. INTRODUCTION

The fact that nature ties the real and imaginary components of a complex variable function of frequency inextricably together, when the variable represents some physically real quantity or phenomena, has been recognized to varying degrees for nearly half a century. For example, Kramers[1] in 1927 noted the general relations between the refractive index and absorption resulting from the simple relationships to the real and imaginary parts of a complex dielectric constant. Because one of the relations was contained in an earlier paper of Kronig's,[2] this relationship is commonly known in the physical science world as the Kramers-Kronig relation. The awareness of the relationship between

the real and imaginary parts of the impedance of an electrical network emerged about the same time as the Kramers-Kronig work.[3,4]

The usefulness of a quantitative solution to the general real and imaginary component relationship was soon recognized. Bode has provided us with a key to the solution of this problem (Ref. 5, Ch. XIV). He gives general integral equations relating the two components, but points out what many have since discovered, namely, that the general integrals can be readily evaluated for only the simplest of functions. Bode, however, presents a practical numerical integration technique for summing the imaginary component associated with a multiple straight-line approximation to the real component as a function of frequency (Ref. 5, Ch. XV). The accuracy of this summation is limited only by the number of straight lines used to approximate the true real component and the accuracy to which the imaginary contribution of each of the straight line segments to the total imaginary component is known. The author has published tables for accomplishing this summation at telecommunication and radio frequencies.[6] These tables made possible the computation of the nonlinear phase from which the delay distortion (dispersion) to be expected in a projected transatlantic repeatered submarine telephone cable system was determined and the delay distortion correction required to make existing coaxial cable systems suitable for the transmission of television programs. Van Vleck utilized the Kramers-Kronig relation while studying microwave propagation during World War II to establish that a significant difference in the refractive index of the atmosphere between wavelengths of 3 cm and 1 cm would lead to an unreasonably high absorption, in contradiction with experiment.[7]

The invention of the optical maser and the availability of coherent light directed attention to the possibility of transmission of intelligence beyond the microwave frequencies to the optical frequencies. The realization of the potential usefulness of the numerical imaginary component summation at optical frequencies resulted from a discussion initiated by a colleague, W. L. Faust. This discussion concerned a proposal by Miller and Lopez[8] that the difference in determination of the velocity of light obtained from measurements at optical frequencies and at microwave frequencies could be explained by the difference in delay time experienced by a wave reflected from a high-quality reflecting surface at optical and microwave frequencies. This is a recurrence at optical frequencies of the delay distortion problem which the earlier phase tables were computed to solve at telecommunication frequencies. These tables were, therefore, extended to make possible similar computations at optical frequencies.

A use for this extension soon arose. Bennett,[9] in his analysis of hole burning effects in a He-Ne optical maser, needed the phase associated with an emission line, Gaussian in shape, but truncated due to an increase in RF power to the maser. The extended tables provided the answer to Bennett's problem and the motivation for writing this paper.

This paper will have two objectives. First, it will extend the numerical computation of the imaginary part from the real part or vice versa of a physical complex variable as a function of frequency from telecommunication and radio frequencies to optical and higher frequencies. Secondly, it will describe a mathematical tool which has proved extremely useful in the telecommunications field and which, it is believed, can be equally useful in the physical sciences.

II. THE NUMERICAL PHASE COMPUTATION TECHNIQUE

In all the discussion to follow, the five statements listed below will apply.

(a) Loss, attenuation, gain, or amplitude, all designated as A, and phase, designated as B, will be used interchangeably with real and imaginary parts, respectively. This is because attenuation in nepers, which is equal to $\log_e$ of the magnitude of a complex voltage or current loss ratio, or $\log_e$ of the amplitude of a complex variable expressed in polar form, and their associated polar angles in radians are identically and respectively interchangeable with real part and imaginary part of a complex variable expressed in rectangular coordinates in the numerical computations to be discussed. In communications problems loss in decibels and angle in degrees rather than nepers and radians respectively are in common use. However, if nepers and radians are considered as the basic units and decibels and degrees as derived units, there will be no difficulty.

(b) Since B_c, the phase at $\omega_c = 2\pi f_c$, is given by Bode (Ref. 5, p. 335) as

$$B_c = \frac{1}{\pi} \int_0^\infty \frac{dA}{d\omega} \log_e \left| \frac{\omega + \omega_c}{\omega - \omega_c} \right| d\omega \tag{1}$$

an amplitude characteristic constant from frequency $f = 0$ to $f = \infty$ contributes nothing to the phase. Therefore, a constant amplitude can be added or subtracted from any amplitude characteristic without affecting the associated phase characteristic.

(c) Since frequency, f, appears only as a ratio in (1), all frequencies can be changed in the same ratio without changing the attenuation-phase relationship in magnitude or form.

(d) All frequencies will be considered on a log frequency scale. Linear frequency scale is permitted in the narrow-band summations only because log f and f are linearly related over a very narrow band. A narrow band will be considered one in which the total frequency range of interest is less than 10^{-3} times the center frequency. All other bands will be referred to as broad bands.

(e) As seen from (1) above, the phase is determined from the integrated slope, $dA/d\omega$, of the amplitude characteristic, A. The slope of a given straight line section of a straight-line approximation to an amplitude characteristic will be designated by k, and k will be defined as $(A_n - A_{n-1})$ in nepers divided by $\log_e (f_n/f_{n-1})$ where A_n and A_{n-1} are the amplitudes at frequencies f_n and f_{n-1} respectively on the straight line section. A unit slope designated by $k = 1$ will be one in which there is a change in A of one neper between two frequencies which are in the ratio $e = 2.7183$. When A is expressed in decibels a unit slope is a change of 6.02 decibels per octave or 20 decibels per decade.

2.1 *Phase Summation Using the Semi-infinite Unit Attenuation Slope*

The numerical phase computation is based on a straight-line approximation to the amplitude characteristic, A. A hypothetical attenuation (real part) characteristic plotted on a log frequency scale along with its straight-line approximation is shown in Fig. 1(a). In Fig. 1(b) this straight-line approximation is in turn broken down into the sum of a series of so-called semi-infinite constant slopes of attenuation. A semi-infinite slope is an attenuation characteristic which has a constant magnitude from 0 to some frequency f and a constant slope from f to $f = \infty$. Thus, in Fig. 1(b), the first semi-infinite slope, k_1, has the constant slope k_1 extending from f_0 to ∞ rather than terminating at f_1 as in Fig. 1(a). Beginning at f_1 a semi-infinite slope equal in magnitude to k_1 but opposite in sign adds to the $+k_1$ slope to produce the straight line segment of our amplitude approximation extending from f_0 to f_1. This process is continued until the complete approximation is obtained. The semi-infinite unit ($k = 1$) slope of attenuation or real part is the fundamental element of all the numerical phase summations. The phase associated with a semi-infinite unit slope is given by Bode (Ref. 5, pp. 342–43) as

$$\begin{aligned} B(x_c) &= \frac{1}{\pi}\int_{x=0}^{x=x_c} \log_e \left|\frac{1+x}{1-x}\right| \frac{dx}{x} \\ &= \frac{2}{\pi}\left(x_c + \frac{x_c^3}{9} + \frac{x_c^5}{25} + \cdots\right) \end{aligned} \tag{2}$$

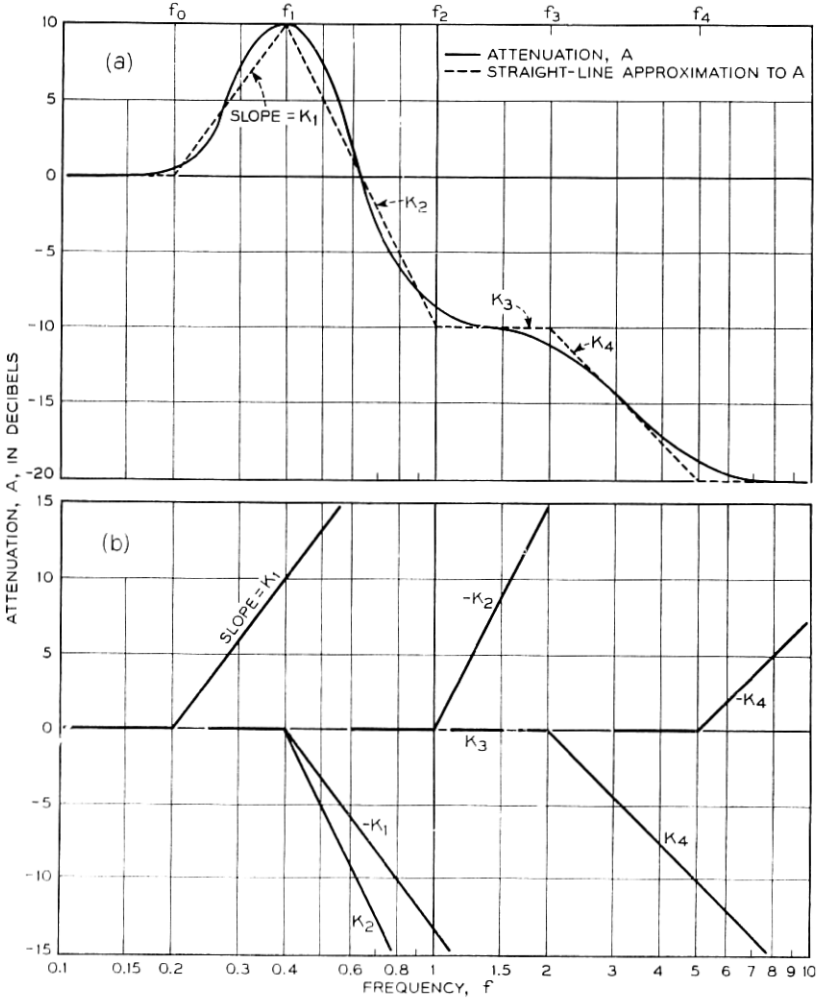

Fig. 1 — (a) Straight-line approximation to attenuation. (b) Semi-infinite slopes which add to produce straight-line approximation.

where $B(x_c)$ is the phase in radians at frequency f_c, $x = f/f_0$, $x_c = f_c/f_0$, $x_c < 1.0$, and f_0 is the frequency at which the unit slope begins.

$B(x_c)$ has a value of 0 at $x_c = 0$, increases monotonically to $\pi/4$ radian at $x_c = 1$, and to $\pi/2$ radians at $x_c = \infty$ with odd symmetry about $x_c = 1$ on a log frequency scale. From the odd symmetry of $B(x_c)$ around $x_c = 1$, $B(x_c')$ for $f_c' > f_0$ is given by

$$B(x_c' = f_0/f_c') = \pi/2 - B(x_c = x_c'). \tag{3}$$

$B(x_c)$ is the function which was tabulated in the tables of Ref. 6.

The phase associated with a semi-infinite slope of magnitude k_n is k_n times $B(x_c)$ of (2). To get the total phase associated with the straight-line approximation and thus with the true amplitude characteristic within the limits of error of the approximation, it is only necessary to sum the phase contributions of each of the semi-infinite slopes making up the straight-line approximation. Thus, the total phase $\theta(f)$ at frequency f is given by

$$\theta(f) = k_1(\theta_0 - \theta_1) + k_2(\theta_1 - \theta_2) + \cdots k_n(\theta_{n-1} - \theta_n) \tag{4}$$

where θ_n is the phase of a semi-infinite unit slope commencing at f_n,

$$k_n = \frac{(A_n - A_{n-1}) \text{ in nepers}}{\log_e (f_n/f_{n-1})} = \frac{(A_n - A_{n-1}) \text{ in decibels}}{20 \log_{10} (f_n/f_{n-1})}. \tag{5}$$

A separate summation must be made for each frequency at which the total phase is desired.

Note the following:

(a) That, as expected, adding or subtracting a constant amplitude to the characteristic does not affect the phase summation of (4).

(b) That initial and final amplitudes need not be the same.

(c) The amplitude need not approach a constant at high or low frequencies but may have a constant slope extending to $f = 0$ or ∞. This is common in electrical networks. A slope extending to ∞ is covered by $B(x_c)$ of (2). The phase of a slope extending to 0 can be read from the $B(x_c)$ tables for the constant slope extending to ∞ by reading the phase for $f/f_0 < 1$ from Table IV designated $f > f_0$ and the phase for $f_0/f < 1$ from Table III designated $f < f_0$ (see Ref. 6, B.S.T.J., p. 881).

Complete step-by-step examples of summing phase using (4) and the tables of phase of a semi-infinite unit attenuation slope are given in Ref. 6.

2.2 *Phase Summation Using the Unit Attenuation Line Segment*

When the value of k_n as given by (5) is substituted in (4), (4) can be rewritten as

$$\theta(f) = \sum_{n=1}^{n} (A_n - A_{n-1}) \frac{\theta_{n-1} - \theta_n}{\log_e (f_n/f_{n-1})} \tag{6}$$

where $(A_n - A_{n-1})$ is the change in amplitude or real part (nepers) on the straight line segment of the approximation to the amplitude characteristic between f_{n-1} and f_n, and $(\theta_{n-1} - \theta_n)/\log_e (f_n/f_{n-1})$ is the phase

contribution of a straight line segment of attenuation or real part having a one-neper change in amplitude between frequencies f_{n-1} and f_n and a constant amplitude below and above f_{n-1} and f_n, respectively. This line segment is identified in its position by the geometric mean of f_{n-1} and f_n, $\sqrt{f_n f_{n-1}}$ and by a slope parameter, a, defined as the ratio of this geometric mean frequency to f_{n-1}.

The "unit line segment" was introduced by Bode (Ref. 5, Ch. XV, Charts V–IX), who gave graphical plots of the phase associated with this element as a function of $x_c = f_c/f_0$ with (a) as a parameter. In a reasonably precise phase summation over a broad band of frequencies, using these charts involves a nonlinear interpolation between curves for different values of a. Therefore, it often proves easier to sum the phase using (4) and the semi-infinite slope charts or tables.

However, in narrow-band problems at optical frequencies, the unit line segment is extremely useful in fast and accurate phase summation. A unit line segment for use with narrow bands is illustrated in Fig. 2. By virtue of the fact that $\log_e f_{12}/f = \log_e (f + \Delta f_{12})/f = \Delta f_{12}/f_{12}$ when $\Delta f_{12} < 10^{-3} f_{12}$, to better than the accuracy to which the amplitude data is likely to be known, a linear frequency plot of amplitude may be used.

The phase of the unit line segment of Fig. 2 will be designated as Φ and will be identified in tabulation by its frequency width Δf and the

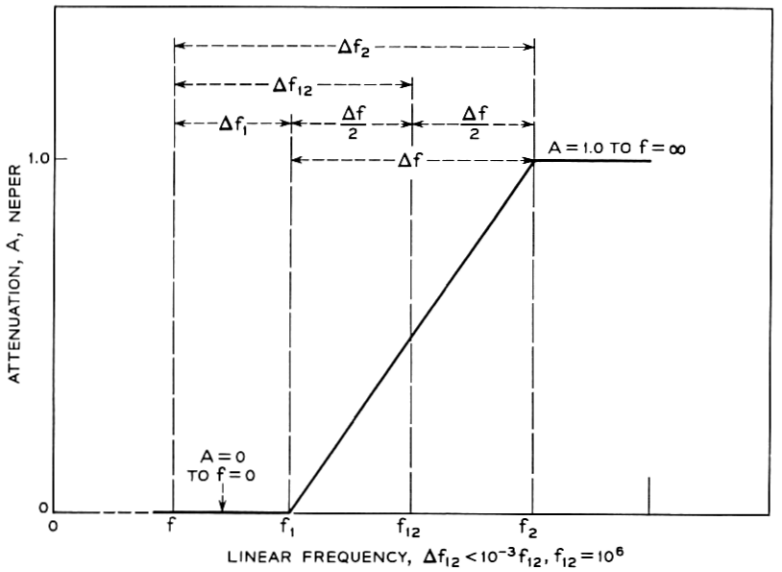

Fig. 2 — Unit attenuation line segment.

difference, Δf_{12}, between its geometric mean frequency $f_{12} = \sqrt{f_1 f_2} = (f_1 + f_2)/2$ and f.

Using unit line segments having a phase contribution of Φ, (6) can now be written

$$\theta(f) = (A_1 - A_0)\Phi_{01} + (A_2 - A_1)\Phi_{12} + \cdots (A_n - A_{n-1})\Phi_{(n-1)n} \quad (7)$$

where $\Phi_{(n-1)n}$ is the phase contribution of a unit attenuation line segment of width $\Delta f = f_n - f_{n-1}$ and a Δf_{12} of $(f_{n-1} + f_n)/2 - f$.

Φ is evaluated in the next section and tabulated in Table V for $f_{12} = 10^6$. Φ is always positive for a positive slope and increases monotonically from 0 at $f = 0$ to a maximum at $f = f_{12}$ beyond which it decreases monotonically to 0 at $f = \infty$. As a function of Δf_{12} it has even symmetry about $\Delta f_{12} = 0$ so that

$$\Phi(\Delta f_{12}) = \Phi(-\Delta f_{12}).$$

Note the restriction of Fig. 2 and of Table V that $f_{12} = 10^6$. This restriction applies *only* if the initial and final values of the amplitude of the characteristic *are not* the same. If they are not the same, the problem must be expanded or contracted about $f = 0$ to a center frequency of 10^6 by multiplying all frequencies by the ratio of 10^6 to the center band frequency. If they are the same, then the problem can be linearly expanded or contracted about its center frequency to best fit the range of Δf_{12} of Table V, and the phase will expand and contract to bear the same relationship to the magnitude. Proof that this is permissible will be given in Section 3.2. If the initial and final values are not the same, they can be made the same by truncating the main high-Q portion of the band from the rest of the band on a constant amplitude line. The phase of the truncated portion having equal initial and final amplitudes can then be summed using the permissible linear expansion or contraction of the band about its center frequency. The residue is then evaluated using the semi-infinite slope summation if the residue becomes a broadband problem. If the residue remains a narrow-band problem, the line segment summation may be used by expanding or contracting about $f = 0$ to make the center frequency equal 10^6. In reassembling the problem and adding the phase of the two parts, the inverse frequency transformations must, of course, be made.

An example of phase summation using the unit line segment phase of Table V in (7) will be given in Section 4.2.

2.3 *Phase Summation Using the Unit Wedge of Attenuation*

The unit wedge of attenuation is a convenient element for very accurate narrow-band phase summation. Although it has been developed

primarily for use with an automatic computer, it is equally useful for rapid but less precise desk computer phase summation.

The summation is limited to characteristics having equal initial and final amplitudes. If they are not equal they can be made so by the division of the problem into two problems by constant amplitude truncation as discussed in Section 2.2.

Since it is assumed that $A_n = A_0$, A_n and A_0 can each be made 0 by subtracting a constant amplitude A_0 from the amplitude characteristic. Equation (7) can then be written:

$$\theta(f) = A_1(\Phi_{01} - \Phi_{12}) + A_2(\Phi_{12} - \Phi_{23}) + \cdots A_{n-1}(\Phi_{(n-2)(n-1)} - \Phi_{(n-1)n}).$$

Each of the terms of the above equation is a magnitude A_n multiplied by the phase difference of two unit line segments of the type illustrated in Fig. 2. The first line segment extends from $f = n - 1$ to $f = n$ and the second from the terminal of the first at $f = n$ to $f = n + 1$. If the widths Δf of these two line segments are equal, they produce the "unit wedge of attenuation," which is the third type of amplitude element used in the numerical phase summation. In using this element the straight-line approximation is limited to equal frequency interval segments. Therefore, the hypothetical problem of Fig. 1 is no longer useful in the discussion and a new problem shown in Fig. 3 will be used. In Fig. 3 the amplitude characteristic is plotted on a linear frequency scale consisting of equally spaced intervals between frequencies which are designated as either f or n. The straight-line approximation is now obtained by taking exact values of A at even values of n on the true

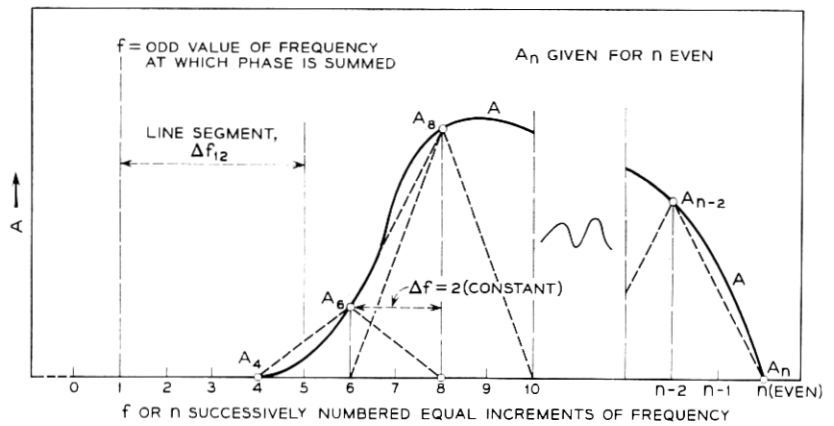

Fig. 3 — Phase summation using wedge element.

amplitude characteristic. Since the accuracy of phase summation is greatest at the midfrequency of the straight line segments approximating the amplitude characteristic, phase will be summed at odd values of n. For rapid desk computing using a less accurate approximation, it may be desirable to take A's which lie off the true curve. This will be covered in Section 4.3.

The total phase at f associated with the full magnitude characteristic of Fig. 3 is then given by the sum of the individual phases contributed by each successive line segment from A_4 to A_6, A_6 to A_8, $\cdots$ A_{n-2} to A_n. Therefore, from (7)

$$\theta(f \text{ odd}) = (A_6 - A_4)\Phi_{\Delta f_{12}=5-f} + (A_8 - A_6)\Phi_{\Delta f_{12}=7-f} + \cdots + (A_{n-2} - A_{n-4})\Phi_{\Delta f_{12}=(n-3)-f} + (A_n - A_{n-2})\Phi_{\Delta f_{12}=(n-1)-f}$$

and since the initial value A_4 and the final value A_n are zero

$$\begin{aligned}\theta(f \text{ odd}) &= A_6(\Phi_{\Delta f_{12}=5-f} - \Phi_{\Delta f_{12}=7-f}) + \cdots \\ &\quad + A_{n-2}(\Phi_{\Delta f_{12}=n-3-f} - \Phi_{\Delta f_{12}=n-1-f}) \\ &= \sum_{n \text{ even}} A_n(\Phi_{\Delta f_{12}=n-(f+1)} - \Phi_{\Delta f_{12}=n-(f+1)+2})\end{aligned} \tag{8}$$

in which the Φ's all have a Δf of 2.

Each term of (8) represents the phase due to a wedge of attenuation in the shape of an isosceles triangle having an amplitude A_n and a base width of 4 frequency intervals. The first of such amplitude elements in Fig. 3 is defined by points ($A = A_4 = 0, f = 4$), ($A_6, f = 6$), and ($A = 0, f = 8$), the second by ($A = 0, f = 6$), ($A_8, f = 8$), and ($A = 0, f = 10$), etc. These amplitudes add to approximate the true curve. When the amplitude A_n is unity, this element is called a unit wedge of attenuation, and its phase contribution is designated by Ψ. Ψ is identified by a subscript which is equal to 500 + its lower frequency line segment's Δf_{12} or by $500 + n - (f + 1)$. The 500 is added to $n - (f + 1)$ to avoid negative subscripts in tabulation. Equation (8) can now be written

$$\theta(f \text{ odd}) = \sum_{n \text{ even}} A_n \Psi_{500+n-(f+1)} \tag{9}$$

where

$$\Psi_{500+n-(f+1)} = \Phi_{\Delta f=2,\, \Delta f_{12}=n-(f+1)} - \Phi_{\Delta f=2,\, \Delta f_{12}=n-(f+1)+2}. \tag{10}$$

Ψ is given in Table VI for $500 + n - (f + 1)$ even from 0 to 1000. In summing phase using (9) the center of the band of the problem is placed at $n = 500$. The band is then linearly expanded or contracted about

$n = 500$ to get a maximum number of amplitude evaluations consistent with the frequency range of the phase summation desired. With Ψ tabulated for $500 + n - (f + 1)$ even from 0 to 1000, the maximum and minimum permissible values of f and n are related as follows

$$500 + f + 1 > n > f + 1 - 500.$$

Thus, for a low value of $n_{\text{even}} = L$ and a high value of $n_{\text{even}} = H$, the phase θ at f can be summed only for odd values of f between $f = H - 501$ and $f = L + 499$.

The ease and accuracy of automatic computer summation of phase using the unit wedge tables and (9) will be demonstrated in Section 4.3. A fast and good phase summation using a less accurate straight-line approximation and a desk computer will also be illustrated.

2.4 *Requirements on the Complex Variable for the Numerical Method to be Applied*

A rigorous discussion of the requirements which must be met by a complex variable if the phase computed from its amplitude characteristic is to represent its true phase is beyond the scope of this paper (see Ref. 5, Ch. XIII). Briefly, it is required that the function be an analytic function of frequency in the right half p ($p = i\omega$) plane and that its real and imaginary components be even and odd functions of frequency, respectively, on the real frequency axis.

Actually, if there is sufficient information available to rigorously determine the applicability of the method, the numerical phase summation technique will usually not be needed. Fortunately, when it is needed the phase summed by the numerical method almost always contains the desired information in spite of the fact that a portion of the phase referred to as nonminimum[5] phase may be missed in the summation. For instance, in a long electrical, optical, acoustical, or other transmission path, where a long path is defined as one in which the length is many multiples of the wavelength of the transmitted signal, there will be an integer multiple of 2π radians which will not be included in the phase summed by the techniques described. However, the phase summed will, in general, contain all of the phase nonlinearity, and in this type of problem the nonlinear phase is usually the phase of interest. Therefore, delay distortion in television transmission lines was successfully delay distortion equalized using phase data obtained by numerical phase summation based on the loss or absorption characteristics of the lines. Also, in Bennett's He-Ne maser problem,[9] the nonlinear phase in the truncated Gaussian line was obtained by nu-

merical phase summation in spite of the fact that an integer multiple of 2π radians in the total phase was missed in the numerical summation.

Similar situations exist with regard to nonminimum imaginary part complex variables where a portion of the imaginary component is missed in the summation. Here again, however, the minimum possible imaginary part associated with the real part which is obtained by the numerical summation, is usually of sufficient interest to make the summation valuable.

There is one important type of nonminimum phase function for which the numerical summation may not be useful. A good example of such a function is an electrical bridge having zero transmission or infinite loss at a real frequency due to bridge balance. This violates the requirement that the function be analytic in the right half p plane. In this case, the phase summed may be the true phase or it may depart radically and nonlinearly from the true phase over a wide frequency band centered at the infinite loss frequency (Ref. 6, B.S.T.J., p. 896). By analogy to the electrical case, the application of the numerical phase summation to optical or other amplitude characteristics having infinite loss obtained by interference (as in an interferometer) or multilayer reflection interference should be approached with caution if not entirely avoided.

2.5 *Computation of Amplitude from Phase*

So far only the determination of phase from amplitude has been considered. The same technique and tables can be used for the reverse computation. However, since a constant amplitude does not change the phase, the amplitude determined from a given phase characteristic must contain an additional arbitrary constant. This is taken into account by considering the attenuation determined as the difference between the true attenuation and the attenuation at either zero or infinity.

In the reverse computation the complex variable $A + iB$ is replaced by either $i\omega(A - A_\infty + iB)$ or $(A - A_0 + iB)/i\omega$. The multiplication by $i\omega$ or its reciprocal has the effect of interchanging the real and imaginary components and their even and odd symmetry characteristics. Thus in $i\omega(A - A_\infty + iB)$, the real component becomes $-\omega B$ with even symmetry and the imaginary component becomes $i\omega(A - A_\infty)$ with odd symmetry. Similarly in $(A - A_0 + iB)/i\omega$, the real component becomes B/ω with even symmetry and the imaginary component becomes $-i(A - A_0)/\omega$ with odd symmetry. The transformed variables are then in suitable form for determining B from A using the same

formula and tables and the same techniques as were described for determining A from B. It must be remembered, of course, that the values of A determined from the summation will include an arbitrary additive constant (Ref. 5, pp. 320–330).

III. COMPUTATION OF PHASE TABLES

3.1 *Semi-Infinite Unit Slope Phase Computation*

The original tables of phase of a semi-infinite slope of Ref. 6 are adequate except for the very steep slopes which may occur at microwave frequencies and frequently occur at optical frequencies. For instance, in the first optical problem to which they were applied, the delay distortion or time dispersion at the surface of a mirror,[10] the critical phase values fell within the final 60 of 9,640 tabulated values of phase in radians falling in the vicinity of $x = f/f_0 = 1.0$. Therefore, the extension of the earlier tables is limited to values of $f/f_0 > 0.9999$. In this region, the best expression for obtaining the phase B is given by Bode as

$$B(x_c) + B(y_c) = \frac{\pi}{4} - \frac{1}{\pi} \log_e x_c \log_e y_c \tag{11}$$

where

$$y_c = \frac{1 - x_c}{1 + x_c}; \qquad x_c = \frac{1 - y_c}{1 + y_c}.$$

From (2)

$$B(x_c) = \frac{2}{\pi}\left[\frac{1 - y_c}{1 + y_c} + \frac{1}{9}\left(\frac{1 - y_c}{1 + y_c}\right)^3 + \cdots\right] = -\frac{1}{\pi} \log_e y_c \tag{12}$$

to better than 2×10^{-14} radian for $(1 - y_c) < 10^{-4}$.

Substituting (12) in (11)

$$B(y_c) = \frac{\pi}{4} + \frac{1}{\pi} \log_e y_c \log_e \frac{e}{x_c}$$

as

$$y_c \to 1.0, \log_e y_c = \frac{2(y_c - 1)}{y_c + 1}$$

and

$$B(y_c) = \frac{\pi}{4} - \frac{2}{\pi}\left[\frac{1 - y_c}{1 + y_c}\log_e \frac{e(1 + y_c)}{1 - y_c}\right]. \tag{13}$$

Equation (13) is good to 3×10^{-13} radian for $y_c > 0.9999$. This equation was used to compute $B(y_c)$ to 12 significant figures for

$$y_c = .99990(.0^41)\ .99998(.0^55)\ .999995(.0^65)$$
$$.999998(.0^62)\ .9999998(.0^61)\ 1.0.$$

These values were then extended by the numerical integration technique described in Ref. 6 to obtain $B(y_c)$ for

$$y_c = .999900(.0^51)\ .999980(.0^65)\ .9999980(.0^62)$$
$$.9999998(.0^61)\ 1.0.$$

These values were then graphically interpolated to obtain 11 significant figure values of $B(y_c)$ for

$$y_c = .999900(.0^51)\ .999980(.0^61)$$
$$.9999998(.0^75)\ 1.0.$$

These final values were rounded to 9 figures to obtain the values given in Table III. The odd symmetry of $B(x_c)$ about $x_c = 1.0$ was used to obtain Table IV in accordance with (3).*

The initial 12-figure computations were good to ± 1 in the 12th figure. The maximum error in numerically integrating and graphically interpolating to 11 significant figures is estimated to be less than 5 figures in the 11th figure. The nine-figure tables are, therefore, believed to be subject only to rounding errors in the last figure.

In order to extend the range of use of Tables III and IV of this paper, values of $B(x_c)$ for $x_c = .9970(.0001)\ .9999$ from the Ref. 6 tables are included.

3.2 *Unit Attenuation Line Segment Phase Computation*

Fig. 2 shows a unit attenuation line segment meeting the restrictions that $\Delta f_{12} < 10^{-3} f_{12}$ and $f_{12} = 10^6$. The phase associated with this amplitude element will be designated as Φ. It is determined by the difference between the phase of a positive semi-infinite slope beginning at $A = 0$ at f_1 and extending to infinity, passing through amplitude $A = 1.0$ at

* Tables of phase functions are numbered the same as tables previously mentioned (Ref. 6). Therefore Tables I and II do not appear in this paper, since angles are given in radians only. Furthermore, additional tabulations in the present paper are numbered consecutively, even though the numbers sometimes duplicate table numbers used in illustrative examples in Ref. 6.

f_2 and the phase of a semi-infinite slope of equal magnitude but opposite in sign beginning at $A = 1.0$ at f_2. In accordance with the definition of slope given by (5), the slope k of these semi-infinite slopes will be

$$k = \frac{A = 1.0}{\log_e f_2/f_1} = \frac{1}{\log_e \dfrac{f_{12} + \Delta f/2}{f_{12} - \Delta f/2}}$$

or

$$1/k = \log_e \frac{1 + \Delta f/2f_{12}}{1 - \Delta f/2f_{12}} = \frac{\Delta f}{f_{12}} \tag{14}$$

to better than 1 in 10^{10} for the maximum value of $\Delta f = 40$ for which Φ will be tabulated. Referring to Fig. 2, Φ will therefore be given by:

$$\Phi = k[B(f/f_1) - B(f/f_2)] \tag{15}$$

$$= (10^6/\Delta f)[B(f/f_1) - B(f/f_2)], f < f_1 \tag{16}$$

$$= (10^6/\Delta f)[B(f_1/f) - B(f/f_2)], f_{12} > f > f_1 \tag{17}$$

in which the B's are the phases of semi-infinite unit slopes of attenuation. Φ need be evaluated only for $f < f_{12}$ since $\Phi(\Delta f_{12}) = \Phi(-\Delta f_{12})$ as a result of the even symmetry of Φ about $f = f_{12}$.

Referring to Fig. 2, when $f < f_1$, f/f_1 is given by

$$f/f_1 = \frac{f_1 - \Delta f_1}{f_1} = 1 - \frac{\Delta f_1}{f_1} = 1 - \frac{\Delta f_{12} - \Delta f/2}{10^6}$$

and $B(f/f_1)$ of (16) is read from Table III for $f < f_0$. When $f > f_1$, $f_1/f = 1 - [(\Delta f/2 - \Delta f_{12})/10^6]$ and $B(f_1/f)$ of (17) is read from Table IV for $f > f_0$. Since $f < f_{12} < f_2$, $f/f_2 = 1 - [(\Delta f_{12} + \Delta f/2)/10^6]$ and $B(f/f_2)$ of (16) and (17) is always read from Table III for $f < f_0$.

Equations (16) and (17) and the approximations to f/f_1 and f/f_2 above may be used to evaluate Φ for $\Delta f_{12} < 50$, $\Delta f < 40$ to an accuracy of better than 0.0002 radian. This is sufficient since Φ is only given to 0.001 radian in Table V. These equations were therefore used to compute Φ of Table V for $\Delta f_{12} = 0$ (1) 50 for each of the following Δf's: 2, 4, 6, 10, 20, and 40.

For $\Delta f_{12} > 50$, $\Delta f < 40$, and $f < f_1$, (15) is used to compute Φ. However, the B's are determined from (13) with $y_e = y_1 = f/f_1$, or $y_e = y_2 = f/f_2$. Thus

$$\Phi = k[B(y_1) - B(y_2)]$$

$$= \frac{2f_{12}}{\pi\Delta f}\left[\frac{1 - y_2}{1 + y_2}\log_e \frac{e(1 + y_2)}{1 - y_2} - \frac{1 - y_1}{1 + y_1}\log_e \frac{e(1 + y_1)}{1 - y_1}\right]. \tag{18}$$

The error in Φ as determined from (18) is less than 10^{-7} radian for $y_{12} = f/f_{12} > .999$, $\Delta f < 40$.
Referring to Fig. 2

$$1 - y_2 = 1 - f/f_2 = 1 - \frac{f_2 - \Delta f_2}{f_2} = \frac{\Delta f_2}{f_2}$$

$$1 + y_2 = 1 + \frac{f_2 - \Delta f_2}{f_2} = 2\left(1 - \frac{\Delta f_2}{2f_2}\right)$$

$$1 - y_1 = \frac{\Delta f_1}{f_1}, 1 + y_1 = 2\left(1 - \frac{\Delta f_1}{2f_1}\right).$$

Substituting in (18)

$$\Phi = \frac{2f_{12}}{\pi\Delta f}\left[\frac{\Delta f_2}{2f_2\left(1 - \frac{\Delta f_2}{2f_2}\right)} \log_e \frac{2ef_2\left(1 - \frac{\Delta f_2}{2f_2}\right)}{\Delta f_2} - \frac{\Delta f_1}{2f_1\left(1 - \frac{\Delta f_1}{2f_1}\right)} \log_e \frac{2ef_1\left(1 - \frac{\Delta f_1}{2f_1}\right)}{\Delta f_1}\right] \tag{19}$$

and as shown in the Appendix, (19) can be reduced to:

$$\Phi = \frac{1}{\pi\Delta f}\left[\Delta f_2 \log_e \frac{2ef_{12}}{\Delta f_2} - \Delta f_1 \log_e \frac{2ef_{12}}{\Delta f_1}\right] - \frac{\Delta f_{12}}{2\pi f_{12}} \tag{20}$$

$$(\Delta f < 40,\ 1000 > \Delta f_{12} > 50).$$

The error term $\Delta f_{12}/2\pi f_{12}$ is only 1.6×10^{-4} radian for $\Delta f_{12} = 1000$. Since Φ in Table V is only given to 0.001 radian, this error term is dropped. Φ as given in (20) can then be further reduced, as shown in the Appendix, to

$$\Phi = \frac{1}{\pi}\left[\log_e \frac{2ef_{12}}{\Delta f_2} - \frac{\Delta f_1}{\Delta f} \log_e \frac{\Delta f_2}{\Delta f_1}\right] \tag{21}$$

$$= \frac{\log_e 10}{\pi}\left[\log_{10} e + \log_{10} \frac{2f_{12}}{\Delta f_2} - \frac{\Delta f_1}{\Delta f} \log_{10} \frac{\Delta f_2}{\Delta f_1}\right]. \tag{22}$$

Φ was computed using (22) for $\Delta f = 10$ at $\Delta f_{12} = 50(2)\ 80(5)\ 160(10)\ 300$, and for $\Delta f = 40$ at $\Delta f_{12} = 50(2)\ 100(5)\ 130$. Five figures to the right of the decimal were retained in spite of the fact that the error term of (20) puts an error of as much as 5 in the last figure, since in deriving unit wedge phase from this data, for Φ (Δf_{12}) differences of

$\Delta f_{12} - \Delta f_{12}' = 2$, the difference error is moved out to 3 in the 7th figure. The computed data was then graphically interpolated to give Φ for $\Delta f = 10$ at $\Delta f_{12} = 50(1)\ 300$ and Φ for $\Delta f = 40$ at $\Delta f_{12} = 50(1)\ 130$. The final data was rounded to 3 figures to the right of the decimal and is subject only to rounding errors. In tabulation, however, the $\Delta f = 10$ values are tabulated for $\Delta f \leqq 20$ at $\Delta f_{12} = 50(1)\ 130$ and for $\Delta f \leqq 40$ at $\Delta f_{12} = 130(1)\ 300$. This introduces a maximum error for the tabulation of 0.0015 radian for $\Delta f = 20$, $\Delta f_{12} = 50$ and 0.0011 radian for $\Delta f = 40$, $\Delta f_{12} = 130$ to give a maximum percentage error in Φ as tabulated between Δf_{12}'s of 50 and 300 of 0.05 per cent.

For $\Delta f_{12} > 300$ it is shown in the Appendix that (21) can be reduced to

$$\Phi = \frac{1}{\pi} \log_e \frac{2f_{12}}{\Delta f_{12}} + \frac{1}{24\pi} \left(\frac{\Delta f}{\Delta f_{12}} \right)^2 \qquad (23)$$

$$(\Delta f < 40,\ 1000 > \Delta f_{12} > 300)$$

The error term $(1/24\pi)(\Delta f/\Delta f_{12})^2$ has a maximum at $\Delta f = 40$, $\Delta f_{12} = 300$ of 2.3×10^{-4} and can be neglected. Equation (23) can then be written for $f_{12} = 10^6$

$$\Phi = \frac{\log_e 10}{\pi} \left(6.0 - \log_{10} \frac{\Delta f_{12}}{2} \right) \qquad (24)$$

$$(\Delta f < 40,\ 1000 > \Delta f_{12} > 300).$$

Equation (24) was used to compute Φ for $\Delta f \leqq 40$ at $\Delta f_{12} = 300(10)\ 1000$ as tabulated in Table V.

One other source of error must be considered. In using the tables the actual center of the line segment being summed will not be at $f_{12} = 10^6$ but may depart from this by half the band spread of the problem. For a band of 10^3 this will be 500. Equation (23) may be used to evaluate this error. It will be given by

$$\text{Max } f_{12} \neq 10^6 \text{ error} = \frac{1}{\pi} \log_e \frac{2f_{12}}{\Delta f_{12}} - \frac{1}{\pi} \log_e \frac{2f_{12} \pm 500}{\Delta f_{12}}$$

$$= \frac{1}{\pi} \log_e \frac{2f_{12}}{2f_{12} \pm 500} = \pm \frac{500}{2\pi f_{12}} < 10^{-4} \text{ radian}$$

which is acceptable for our tabulation.

Recapitulating, the Table V phase values may be considered to be reliable to ± 0.002 radian or less than 0.1 per cent, which is better than the amplitude approximations which are usually used for the unit attenuation line segment phase summation.

The reason for the restriction on center-band frequency in line segment phase summation when the initial and final amplitudes are not the same is now apparent. f_{12} appears as a factor term in all equations for Φ. Since Φ was computed for $f_{12} = 10^6$, the problem must be transformed to a center frequency of 10^6 by multiplying all frequencies by the ratio of 10^6 to the actual center frequency. This does not change the attenuation-phase relationship, since all frequency terms in the Φ expression appear as ratios.

Now consider the problem when the initial and final amplitudes are the same, as shown in the hypothetical problem of Fig. 4. Note that the entire amplitude characteristic can be constructed of trapezoidal elements by successive constant amplitude truncations. A typical element is *abcd*. Its phase at f is given by the sum of the phases of the two line segments *ab* and *cd*. Thus:

$$\Phi(f) \text{ of } abcd = A_{ab}[\Phi(\Delta f_{12}) - \Phi(\Delta f_{34})] \tag{25}$$

and from (21)

$$\begin{aligned}
\Phi(\Delta f_{12}) - \Phi(\Delta f_{34}) &= \frac{1}{\pi}\left[\log_e \frac{2ef_{12}}{\Delta f_2} - \frac{\Delta f_1}{\Delta f_a}\log_e \frac{\Delta f_2}{\Delta f_1}\right. \\
&\qquad \left. - \log_e \frac{2ef_{34}}{\Delta f_4} + \frac{\Delta f_3}{\Delta f_b}\log_e \frac{\Delta f_4}{\Delta f_3}\right] \\
&= \frac{1}{\pi}\left[\log_e \frac{2ef_{12}}{\Delta f_2}\,\frac{\Delta f_4}{2e(f_{12}+F)}\right. \\
&\qquad \left. - \frac{\Delta f_1}{\Delta f_a}\log_e \frac{\Delta f_2}{\Delta f_1} + \frac{\Delta f_3}{\Delta f_b}\log_e \frac{\Delta f_4}{\Delta f_3}\right] \\
&= \frac{1}{\pi}\left[\log_e \frac{\Delta f_4}{\Delta f_2} - \frac{\Delta f_1}{\Delta f_a}\log_e \frac{\Delta f_2}{\Delta f_1}\right. \\
&\qquad \left. + \frac{\Delta f_3}{\Delta f_b}\log_e \frac{\Delta f_4}{\Delta f_3}\right] - \frac{F}{\pi f_{12}}.
\end{aligned} \tag{26}$$

$F/f_{12} < 10^{-3}$ by the narrow-band limitation of our problem, so the second term of (26) is less than 0.0003 radian, which is negligible. Note that f_{12} has disappeared from the first term and that the phase is now dependent only upon ratios of linear frequency intervals. Although f was chosen $< f_1$ in obtaining (26), the dependence of $\Phi(\Delta f_{12}) - \Phi(\Delta f_{34})$ on ratios of linear frequency intervals only, can be shown for all values of f. The problem can, therefore, be linearly expanded or contracted about its center frequency to best fit the range of tabulated values of Φ with-

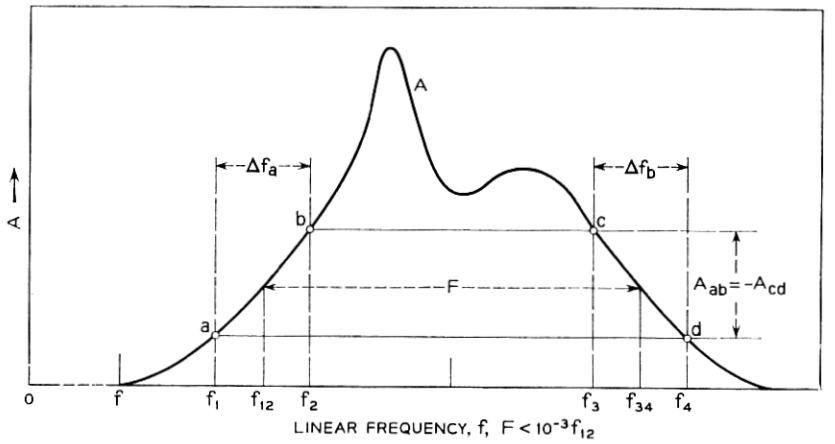

Fig. 4 — Line segment phase summation.

out changing the attenuation-phase relationship, as noted earlier in Section 2.2.

3.3 *Unit Wedge Phase Computation*

The phase contribution of a unit wedge of attenuation is given by (10) as

$$\Psi_{500+n-(f+1)} = \Phi_{\Delta f_{12}=n-(f+1)} - \Phi_{\Delta f_{12}=n-(f+1)+2}$$

where $\Delta f = 2$ for both Φ's and n and f are even and odd integers respectively. If f of (10) is $n + b$ then

$$\Psi_{500-(b+1)} = \Phi_{\Delta f_{12}=-(b+1)} - \Phi_{\Delta f_{12}=-b+1}. \tag{27}$$

If f of (10) is $n - b$ then

$$\Psi_{500+b-1} = \Phi_{\Delta f_{12}=b-1} - \Phi_{\Delta f_{12}=b+1}. \tag{28}$$

Because of the even symmetry of Φ about $f = f_{12}$ and therefore about $\Delta f_{12} = f - f_{12} = 0$,

$$\Phi_{\Delta f_{12}=-(b+1)} = \Phi_{\Delta f_{12}=b+1}$$

and

$$\Phi_{\Delta f_{12}=-b+1} = \Phi_{\Delta f_{12}=b-1}.$$

Therefore, from (27) and (28)

$$\Psi_{499-b} = -\Psi_{499+b}. \tag{29}$$

$\Psi_{500+n-(f+1)}$ for $500 + n - (f + 1)$ even from 500 to 600 was computed using the 11-figure tables of $B(x_c)$ — before reduction to 9 figures for tabulation — to compute the Φ values needed in (10). The Φ values were computed in accordance with the procedure given in Section 3.2 for Φ ($\Delta f < 40$, $\Delta f_{12} < 50$). The extension of this Φ computation to $\Delta f_{12} = 100$ is permissible because of the small value of $\Delta f = 2$. The use of 11-figure tables of $B(x_c)$ good to only five in the final figure is permissible because small differences ($\Delta f = 2$) in this table are good to at least one more significant figure. The final figure in the tabulated values of Ψ depends upon differences in the 11th figure in $B(x_c)$. They are, therefore, estimated to be good to better than ± 2 in the last figure.

$\Psi_{500+n-(f+1)}$ for $500 + n - (f + 1)$ even from 600 to 1000 was computed using 5 decimal figure values of Φ computed before rounding for tabulation in accordance with the procedure given in Section 3.2 for $1000 > \Delta f_{12} > 50$. In accordance with the discussion of the reliability of these computations in Section 3.2, the resultant 5-decimal figures of Ψ are estimated to be reliable to better than ± 2 in the final figure. Values of $\Psi_{500+n-(f+1)}$ for $500 + n - (f + 1) < 500$ were obtained from the values for $500 + n - (f + 1) \geqq 500$ using (29).

Table VI, giving $\Psi_{500+n-(f+1)}$ for $500 + n - (f + 1)$ even from 0 to 1000 to 5 decimal figures, was tabulated using the above data.

IV. EXAMPLES OF PHASE SUMMATION

4.1 *Semi-Infinite Unit Slope Phase Summation*

Summation of phase using the semi-infinite slope of attenuation is described in Section 2.1 and fully illustrated in Ref. 6. Therefore, an actual numerical summation is not considered necessary here.

4.2 *Unit Line Segment Phase Summation*

A part of the truncated Gaussian problem solved for Bennett[9] will be used to illustrate unit line segment phase summation. Fig. 5(a) shows the top portion of a Gaussian amplitude characteristic, A, normalized to a peak amplitude of unity and truncated at $A = 0.712$ and $A = 0.5$.

The characteristic has a half width at half maximum of 800 mc, corresponding to the full Doppler width at half maximum for neon atoms at the temperature of the He-Ne optical maser. It has a center frequency of approximately 2.6×10^{14} cps, corresponding to the frequency of oscillation of the maser. Since the ratio of the bandwidth to

center frequency is ten orders of magnitude smaller than the narrow-band requirement, and the initial and final amplitudes of the truncated section are the same, a linear frequency summation scale was chosen for convenience in unit line segment summation as shown on Fig. 5(a).

The phase wanted is the phase due to that portion of the Gaussian lying between $A = 0.5$ and $A = 0.712$. Since the two sides of this area which are defined by the Gaussian are essentially straight lines, the characteristic was approximated by the two straight lines, ac and $c'e$, and the three constant amplitude lines $A = 0.712$ from c to c', $A = 0.5$ from $f_T = 0$ to $f = 0$, and $A = 0.5$ from $f = 80$ to $f_T = \infty$. This approximation was then broken into four line segments, ab, bc, $c'd$, and de. The desired phase is then given by (7) as

$$\theta(f) = (A_b - A_a)\Phi_{ab} + (A_c - A_b)\Phi_{bc} + (A_d - A_{c'})\Phi_{c'd} + (A_e - A_d)\Phi_{de}$$

and since

$$\begin{aligned}(A_b - A_a) &= (A_c - A_b) = -(A_d - A_{c'}) = -(A_e - A_d) \\ &= 0.106 \text{ neper}, \qquad (30) \\ \theta(f) &= 0.106[\Phi_{ab} + \Phi_{bc} - \Phi_{c'd} - \Phi_{de}] \text{ radians}.\end{aligned}$$

From Fig. 5, $\Delta f = 6$ for all the line segments, and

ab has a center frequency of 3 and its $\Delta f_{12} = |(3 - f)|$,

bc has a center frequency of 9 and its $\Delta f_{12} = |(9 - f)|$,

$c'd$ has a center frequency of 71 and its $\Delta f_{12} = |(71 - f)|$,

de has a center frequency of 77 and its $\Delta f_{12} = |(77 - f)|$.

Table VII gives the entire tabulation and phase summation of (30). The first column gives frequency, f, at which phase is to be summed. The second column gives Δf_{12} for line ab at each value of f, and the third column gives Φ_{ab} for $\Delta f = 6$ from Table V for each value of Δf_{12} at f. This is repeated for Φ_{bc}, $\Phi_{c'd}$, and Φ_{de}. Note the orderly recurrence of values of Φ, which made for easy tabulation.

A desk computer was used to sum the four unit line segment phase contributions horizontally [$\Phi_{c'd}$ and Φ_{de} negatively from (30)] and then multiply the sum by 0.106 to get $\theta(f)$ of the last column in radians. This summed phase is plotted as B on Fig. 5(b). The precision of the summation is demonstrated by the smoothness of the data.

The ease of the computation is illustrated by the fact that the approximation and phase summation was completed in one hour.

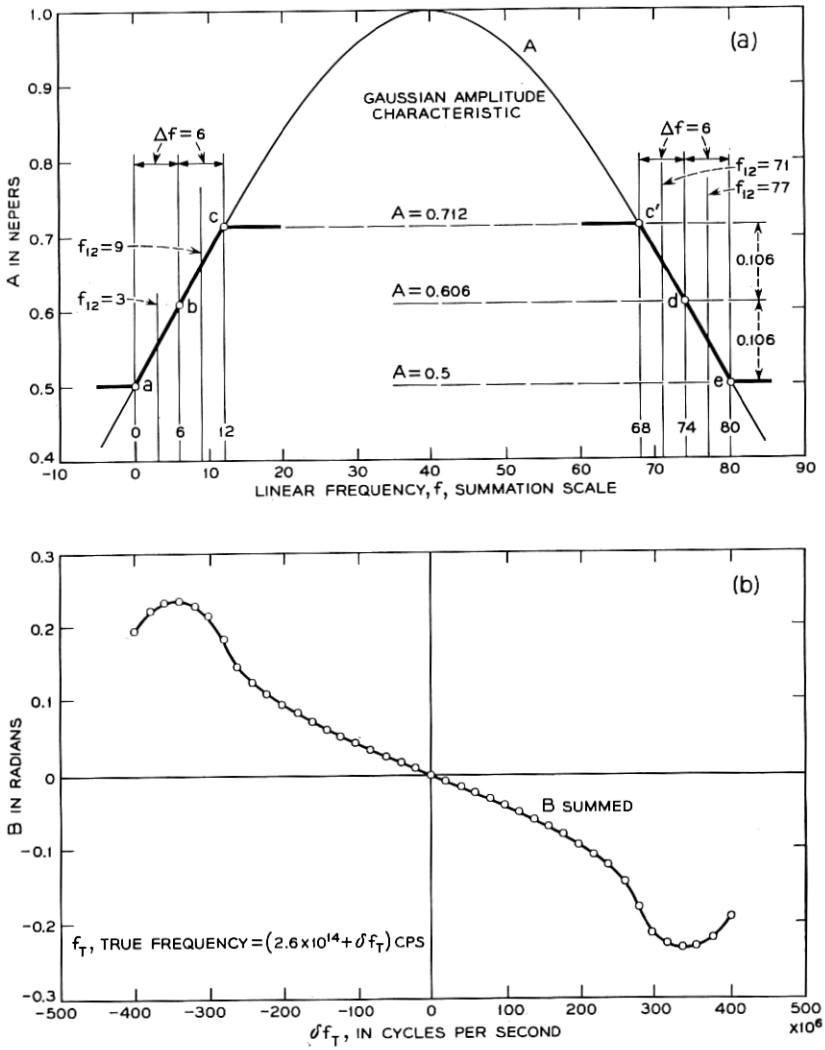

Fig. 5 — (a) Double truncated Gaussian amplitude characteristic. (b) Phase determined by unit line segment summation.

4.3 *Unit Wedge Phase Summation*

The quantum-mechanically derived expression for the complex dielectric constant, $\epsilon = \epsilon_1 - i\epsilon_2$, will be used to illustrate phase summation using the unit wedge for three reasons.

First, ϵ is defined by a Lorentzian whose real and imaginary parts are known. Phase summation of ϵ can therefore be checked against known data. Secondly, it is derivable from the classical equation for a damped harmonic oscillator which occurs repeatedly in science and engineering.[11] Finally, the real part of ϵ is summed from the imaginary part and serves to illustrate the reverse summation discussion in Section 2.5.

The formula for complex dielectric constant given by Van Vleck (Ref. 7, p. 644) can be written as the sum of two Lorentzians as follows

$$\epsilon - 1 = A - \frac{A}{2}\left\{\frac{\nu}{(\nu - \nu_0) - i\Delta\nu} + \frac{\nu}{(\nu + \nu_0) - i\Delta\nu}\right\} \tag{31}$$

where ν = frequency (f), $\Delta\nu$ = half bandwidth at $|\epsilon - 1| = 0.5$ maximum, and A is a constant.

For a narrow band about ν_0 only the first term of (31) is important and (31) can therefore be written

$$\epsilon - 1 = A - \frac{A\nu_0}{2}\left\{\frac{1}{(\nu - \nu_0) - i\Delta\nu}\right\}. \tag{32}$$

From (31), A is seen to be $\epsilon_0 - 1$ where $\epsilon_0 = \epsilon(\nu = 0)$. Substituting for the isolated A term in (32), and separating into real and imaginary parts (32) becomes

$$(\epsilon_1 - \epsilon_0) - i\epsilon_2 = \frac{A\nu_0}{2}\left[\frac{(\nu_0 - \nu)}{(\nu - \nu_0)^2 + \Delta\nu^2} - i\,\frac{\Delta\nu}{(\nu - \nu_0^2)^2 + \Delta\nu^2}\right]. \tag{33}$$

It is desired to obtain refraction from absorption, and the absorption term is in the imaginary part of (33). Therefore real and imaginary must be reversed by multiplying by $i\omega$ or $i2\pi\nu$ as discussed in Section 2.5. Since $2\pi\nu$ is effectively constant across a narrow band, (33) need only be multiplied by i to obtain

$$\epsilon_2 + i(\epsilon_1 - \epsilon_0) = \frac{A\nu_0}{2}\left[\frac{\Delta\nu}{(\nu - \nu_0)^2 + \Delta\nu^2} + i\,\frac{\nu_0 - \nu}{(\nu - \nu_0)^2 + \Delta\nu^2}\right]. \tag{34}$$

Multiplying (34) by $1/\Delta\epsilon$ where $\Delta\epsilon = A\nu_0/2\Delta\nu$, a constant which does not change the real-imaginary relationship, (34) becomes

$$\frac{\epsilon_2}{\Delta\epsilon} + i\,\frac{(\epsilon_1 - \epsilon_0)}{\Delta\epsilon} = \frac{\Delta\nu^2}{(\nu - \nu_0)^2 + \Delta\nu^2} + i\,\frac{\Delta\nu(\nu_0 - \nu)}{(\nu - \nu_0)^2 + \Delta\nu^2}. \quad (35)$$

Van Vleck plots $(\epsilon_2/\Delta\epsilon)2\pi \log_{10} e$ and $(\epsilon_1 - \epsilon_0)/\Delta\epsilon$ in his atmospheric absorption study at microwave frequencies (Ref. 7, Fig. 8.2). Equation (35) is also identical with the expression for the impedance of a parallel RLC circuit having a half width of Δf which shows the recurrence of the damped harmonic oscillator problem noted above.

The real and imaginary parts of (35), hereafter designated as A and B, respectively, were arithmetically computed to four significant figures for $\nu_0 = 10^6$, $\Delta\nu^2 = 10^3$. A and B are plotted in Fig. 6(a) on an f (also n) scale chosen for summation convenience in summing by (9). Because of the even and odd symmetry of A and B respectively about the center frequency, only half of the curves are shown.

Amplitude A data for phase summation were taken for n even from 250 to 750 from the four figure computed values of A. However A was cut off linearly from $A = 0.016$ at $n = 258$ to $A = 0$ at $n = 250$, even though A was decreasing very slowly for $n < 250$. In accordance with Section 2.3, phase can then be summed between $f = 249$ and 749 odd. Equation (9) then becomes

$$B(f = 249 \text{ to } 749 \text{ odd}) = \sum_{\substack{n=250 \\ \text{even}}}^{750} A_n \Psi_{500+n-(f+1)} \quad (36)$$

$B(f)$ of (36) was summed on the 7090 computer.

The difference between $B(f)$ summed and four-figure $B(f)$ computed from (35) are plotted as the "Error in Radians — Precision Summation" in Fig. 6(b). The maximum error between $f = 419$ and 499 is only 0.001 radian. For $f < 419$, the error gradually increases. This is due to the arbitrary cutoff of A at $n = 250$ noted above. If a correction is made for this cutoff, the error at $f = 369$ drops from point $a = +0.0022$ radian to point $b = 0.0002$ radian [see Fig. 6(b)]. This shows that the potential overall accuracy of the phase summation is equal to the accuracy of the amplitude data.

In order to illustrate the accuracy of an order of magnitude poorer approximation to A, the summation frequency scale was reduced by a factor of 10 to the scale for f or n marked "Desk Computer Summation." Now A changes an order of magnitude more in frequency interval of $\Delta f = 2$ then on the precision f or n scale. Therefore a better approximation to A is sometimes obtained by taking straight line terminal points off the true A curve. The points selected are indicated and several of the resultant line segments making up the approximation are shown in dotted lines.

The summation performed was

$$\theta(f = 491 \text{ to } 499 \text{ odd}) = \sum_{\substack{n=480 \\ \text{even}}}^{520} A_n \Psi_{500+n-(f+1)} .$$

This summation required 30 minutes with a desk computer and produced the good approximation to the true phase shown on Fig 6(a).

V. VALUE OF THE NUMERICAL PHASE SUMMATION TECHNIQUE

A knowledge of the imaginary as well as the real part of experimentally observed physical phenomena adds a new dimension to the understanding of the phenomena especially when the physical mechanisms involved are only partially understood. Consider for instance the difficulty of solving the time dispersion of reflection at the surface of a mirror as discussed in Ref. 9. This problem was easily solved using the phase tables, with no need for a quantitative knowledge of the physical mechanisms involved.

When the phenomena can be represented by a Lorentzian or Gaussian, as is often the case, the numerical solution of phase is not necessary. For instance a Lorentzian approximation to the common-base current gain of a transistor revealed that the high common-emitter current gain is obtained at the price of a corresponding loss in frequency band.[12] However this approximation was not good enough for later study of VHF transistors. Here a knowledge of the numerical relationship between amplitude and phase made possible an understanding of current gain and phase from simple amplitude measurements only. The results not only prove good for all types of junction transistors but also reveal rather than require information on the gradient of the base layer impurity distribution.[13] And the computations of delay distortion mentioned in the introduction, although theoretically possible, would have been extremely difficult without a knowledge of the numerical computation of phase.

Finally, consider the potential range of usefulness of the phase tables. It is believed that the phase tables presented in Ref. 6 combined with the phase tables of this paper are sufficient to sum the phase of any minimum phase function occurring in any area of the physical or engineering sciences and in any part of the frequency spectrum.

VI. ACKNOWLEDGMENTS

The author is particularly indebted to Hendrik W. Bode, whose basic theoretical work and straight-line approximation method provided the

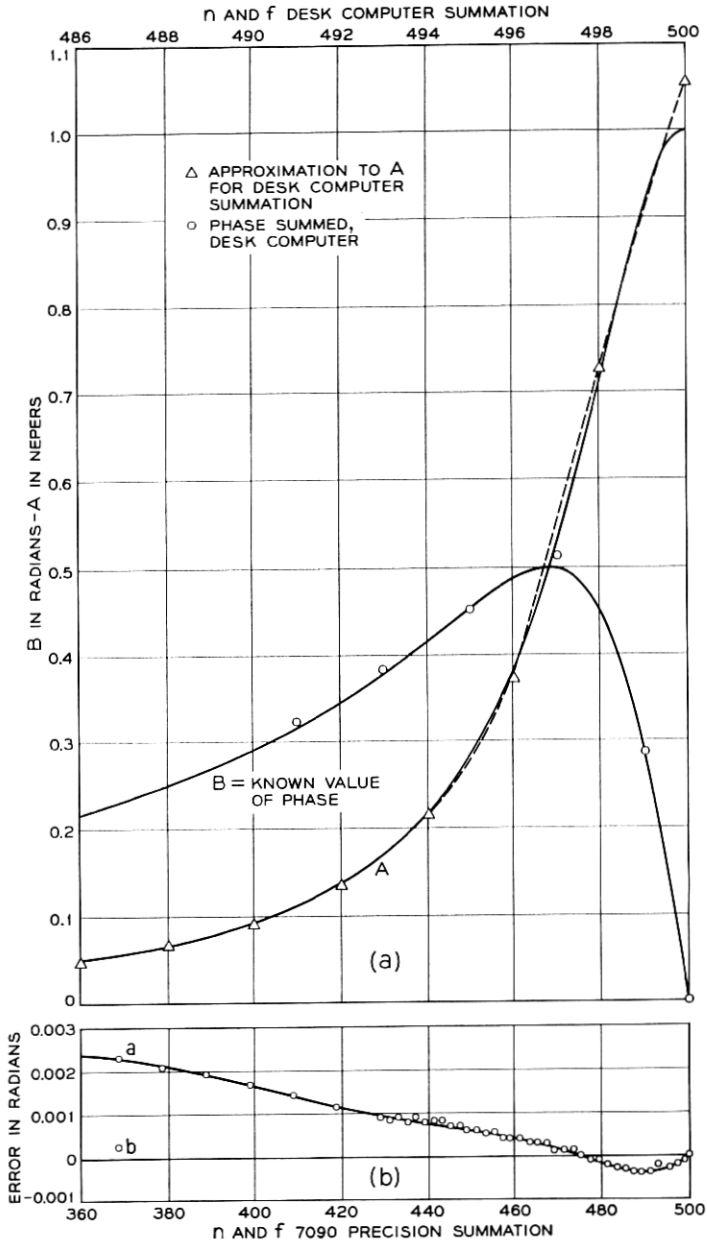

Fig. 6 — (a) Lorentzian line $A + jB = (\epsilon_2/\Delta\epsilon) + i[(\epsilon_1 - \epsilon_0)/\Delta\epsilon]$. (b) Error in precision phase summation using the unit wedge.

foundation for the entire development of the precision numerical phase summation technique. He also wishes to thank W. L. Faust, whose discussions with the author led to a realization of the potential usefulness of the method at optical frequencies; W. R. Bennett, Jr., whose He-Ne maser mode splitting analysis demonstrated the usefulness of the method; Miss Ruth A. Weiss for programming and following through computations of narrow-band summation; J. M. Klein for carrying out a large part of the numerical computations of the new tables; and D. E. McCumber and C. G. B. Garrett for helpful discussions during the writing of this paper.

APPENDIX

Equation (19) of Section 3.2 is reduced to (20) as follows: leaving out the coefficient $2f_{12}/\pi\Delta f$ and treating only the portion in brackets

$$\left[\frac{\Delta f_2}{2f_2\left(1-\frac{\Delta f_2}{2f_2}\right)}\log_e\frac{2ef_2\left(1-\frac{\Delta f_2}{2f_2}\right)}{\Delta f_2}\right.$$

$$\left.-\frac{\Delta f_1}{2f_1\left(1-\frac{\Delta f_1}{2f_1}\right)}\log_e\frac{2ef_1\left(1-\frac{\Delta f_1}{2f_1}\right)}{\Delta f_1}\right]$$

$$=\left[\frac{\Delta f_2}{2f_{12}\left(1+\frac{\Delta f}{2f_{12}}\right)\left(1-\frac{\Delta f_2}{2f_{12}}\right)}\log_e\frac{2ef_{12}\left(1+\frac{\Delta f}{2f_{12}}\right)\left(1-\frac{\Delta f_2}{2f_{12}}\right)}{\Delta f_2}\right.$$

$$\left.-\frac{\Delta f_1}{2f_{12}\left(1-\frac{\Delta f}{2f_{12}}\right)\left(1-\frac{\Delta f_1}{2f_{12}}\right)}\log_e\frac{2ef_{12}\left(1-\frac{\Delta f}{2f_{12}}\right)\left(1-\frac{\Delta f_1}{2f_{12}}\right)}{\Delta f_1}\right]$$

$$=\left[\frac{\Delta f_2}{2f_{12}\left(1-\frac{\Delta f_2-\Delta f}{2f_{12}}\right)}\log_e\frac{2ef_{12}\left(1-\frac{\Delta f_2-\Delta f}{2f_{12}}\right)}{\Delta f_2}\right.$$

$$\left.-\frac{\Delta f_1}{2f_{12}\left(1-\frac{\Delta f_1+\Delta f}{2f_{12}}\right)}\log_e\frac{2ef_{12}\left(1-\frac{\Delta f_1+\Delta f}{2f_{12}}\right)}{\Delta f_1}\right]$$

$$= \left[\frac{\Delta f_2 \left(1 + \frac{\Delta f_1}{2f_{12}}\right)}{2f_{12}} \log_e \frac{2ef_{12}\left(1 - \frac{\Delta f_1}{2f_{12}}\right)}{\Delta f_2} \right.$$

$$\left. - \frac{\Delta f_1 \left(1 + \frac{\Delta f_2}{2f_{12}}\right)}{2f_{12}} \log_e \frac{2ef_{12}\left(1 - \frac{\Delta f_2}{2f_{12}}\right)}{\Delta f_1} \right]$$

$$= \frac{\Delta f_2}{2f_{12}} \left(1 + \frac{\Delta f_1}{2f_{12}}\right) \left(-\frac{\Delta f_1}{2f_{12}} + \log_e \frac{2ef_{12}}{\Delta f_2} \right)$$

$$\left. - \frac{\Delta f_1}{2f_{12}} \left(1 + \frac{\Delta f_2}{2f_{12}}\right) \left(-\frac{\Delta f_2}{2f_{12}} + \log_e \frac{2ef_{12}}{\Delta f_1} \right) \right]$$

$$= \left[\frac{\Delta f_2}{2f_{12}} \left\{ \log_e \frac{2ef_{12}}{\Delta f_2} + \frac{\Delta f_1}{2f_{12}} \left(1 + \log_e \frac{2f_{12}}{\Delta f_2} - 1\right) \right\} \right.$$

$$\left. - \frac{\Delta f_1}{2f_{12}} \left\{ \log_e \frac{2ef_{12}}{\Delta f_1} + \frac{\Delta f_2}{2f_{12}} \left(1 + \log_e \frac{2f_{12}}{\Delta f_1} - 1\right) \right\} \right]$$

$$= \left[\frac{\Delta f_2}{2f_{12}} \log_e \frac{2ef_{12}}{\Delta f_2} - \frac{\Delta f_1}{2f_{12}} \log_e \frac{2ef_{12}}{\Delta f_1} \right]$$

$$+ \left[\frac{\Delta f_2 \Delta f_1}{(2f_{12})^2} \log_e \frac{2f_{12}}{\Delta f_2} - \frac{\Delta f_2 \Delta f_1}{(2f_{12})^2} \log_e \frac{2f_{12}}{\Delta f_1} \right].$$

When the above is multiplied by the coefficient $2f_{12}/\pi\Delta f$ it becomes:

$$\frac{1}{\pi\Delta f} \left[\Delta f_2 \log_e \frac{2ef_{12}}{\Delta f_2} - \Delta f_1 \log_e \frac{2ef_{12}}{\Delta f_1} \right] + \frac{\Delta f_1 \Delta f_2}{2\pi \Delta f f_{12}} \log_e \frac{\Delta f_1}{\Delta f_2}$$

$$= \frac{1}{\pi\Delta f} \left[\Delta f_2 \log_e \frac{2ef_{12}}{\Delta f_2} - \Delta f_1 \log_e \frac{2ef_{12}}{\Delta f_1} \right] + \frac{\Delta f_1 \Delta f_2}{2\pi \Delta f f_{12}} \log_e \frac{\Delta f_{12} - \frac{\Delta f}{2}}{\Delta f_{12} + \frac{\Delta f}{2}}$$

$$= \frac{1}{\pi\Delta f} \left[\Delta f_2 \log_e \frac{2ef_{12}}{\Delta f_2} - \Delta f_1 \log_e \frac{2ef_{12}}{\Delta f_1} \right] - \frac{{\Delta f_{12}}^2}{2\pi \Delta f f_{12}} \times \frac{\Delta f}{\Delta f_{12}}$$

$$(\Delta f < 40, \quad 1000 > \Delta f_{12} > 50)$$

$$= \frac{1}{\pi\Delta f} \left[\Delta f_2 \log_e \frac{2ef_{12}}{\Delta f_2} - \Delta f_1 \log_e \frac{2ef_{12}}{\Delta f_1} \right] - \frac{\Delta f_{12}}{2\pi f_{12}}$$

$$(\Delta f < 40, \quad 1000 > \Delta f_{12} > 50)$$

which is the value of Φ given in (20). The first term of (20) can be further reduced as follows

$$\frac{1}{\pi\Delta f}\left[\Delta f_2 \log_e \frac{2ef_{12}}{\Delta f_2} - \Delta f_1 \log_e \frac{2ef_{12}}{\Delta f_1}\right]$$

$$= \frac{1}{\pi\Delta f}\left[(\Delta f_1 + \Delta f) \log_e \frac{2ef_{12}}{\Delta f_2} - \Delta f_1 \log_e \frac{2ef_{12}}{\Delta f_1}\right]$$

$$= \frac{1}{\pi\Delta f}\left[\Delta f \log_e \frac{2ef_{12}}{\Delta f_2} - \Delta f_1 \log_e \frac{2ef_{12}}{\Delta f_1} \times \frac{\Delta f_2}{2ef_{12}}\right]$$

$$= \frac{1}{\pi}\left[\log_e \frac{2ef_{12}}{\Delta f_2} - \frac{\Delta f_1}{\Delta f} \log_e \frac{\Delta f_2}{\Delta f_1}\right]$$

which is the value of Φ given in (21).

Equation (21) can be still further reduced for $\Delta f_{12} > 300$ as follows. Leaving the factor $1/\pi$ and taking only the bracketed terms of (21)

$$\log_e \frac{2ef_{12}}{\Delta f_2} - \frac{\Delta f_1}{\Delta f} \log_e \frac{\Delta f_2}{\Delta f_1}$$

$$= \log_e \frac{2ef_{12}}{\Delta f_{12}\left(1 + \dfrac{\Delta f}{2\Delta f_{12}}\right)} - \frac{\Delta f_1}{\Delta f} \log_e \frac{\Delta f_{12} + \dfrac{\Delta f}{2}}{\Delta f_{12} - \dfrac{\Delta f}{2}}$$

$$= \log_e \frac{2ef_{12}}{\Delta f_{12}} - \log_e\left(1 + \frac{\Delta f}{2\Delta f_{12}}\right) - \left(\frac{\Delta f_{12}}{\Delta f} - \frac{1}{2}\right)\left[\log_e\left(1 + \frac{\Delta f}{2\Delta f_{12}}\right) - \log_e\left(1 - \frac{\Delta f}{2\Delta f_{12}}\right)\right]$$

$$= \log_e \frac{2ef_{12}}{\Delta f_{12}} - \frac{\Delta f}{2\Delta f_{12}} + \frac{1}{2}\left(\frac{\Delta f}{2\Delta f_{12}}\right)^2 - \frac{1}{3}\left(\frac{\Delta f}{2\Delta f_{12}}\right)^3 + \cdots$$

$$- \left(\frac{\Delta f_{12}}{\Delta f} - \frac{1}{2}\right)\left[\begin{array}{l} \dfrac{\Delta f}{2\Delta f_{12}} - \dfrac{1}{2}\left(\dfrac{\Delta f}{2\Delta f_{12}}\right)^2 + \dfrac{1}{3}\left(\dfrac{\Delta f}{2\Delta f_{12}}\right)^3 - \dfrac{1}{4}\left(\dfrac{\Delta f}{2\Delta f_{12}}\right)^4 \\ + \dfrac{\Delta f}{2\Delta f_{12}} + \dfrac{1}{2}\left(\dfrac{\Delta f}{2\Delta f_{12}}\right)^2 + \dfrac{1}{3}\left(\dfrac{\Delta f}{2\Delta f_{12}}\right)^3 + \dfrac{1}{4}\left(\dfrac{\Delta f}{2\Delta f_{12}}\right)^4 \end{array}\right]$$

$$= \log_e \frac{2ef_{12}}{\Delta f_{12}} - \frac{\Delta f}{2\Delta f_{12}} + \frac{1}{2}\left(\frac{\Delta f}{2\Delta f_{12}}\right)^2 - \frac{1}{3}\left(\frac{\Delta f}{2\Delta f_{12}}\right)^3 + \frac{\Delta f}{2\Delta f_{12}} + \frac{1}{3}\left(\frac{\Delta f}{2\Delta f_{12}}\right)^3$$

$$- 1 - \frac{2}{24}\left(\frac{\Delta f}{2\Delta f_{12}}\right)^2$$

$$= \log_e \frac{2f_{12}}{\Delta f_{12}} + \frac{1}{24}\left(\frac{\Delta f}{\Delta f_{12}}\right)^2$$

which when multiplied by $1/\pi$ becomes

$$\frac{1}{\pi}\log_e\frac{2f_{12}}{\Delta f_{12}}+\frac{1}{24\pi}\left(\frac{\Delta f}{\Delta f_{12}}\right)^2$$

which is the expression for Φ in (23).

REFERENCES

1. Kramers, H. A., Atti del Congresso Internationale dei Fisici, Como, **2,** 1927, p. 545.
2. Kronig, R. de L., Jour. Opt. Soc. Am., **12,** 1926, p. 547.
3. Carson, John R., *Electric Circuit Theory and the Operational Analysis*, New York, McGraw-Hill, 1926, p. 180. Also see Bush, Vannevar, *Operational Circuit Analysis*, New York, John Wiley, 1929, p. 180.
4. For an extensive bibliography, see Murakami, T., and Corrington, M. S., RCA Review, **9,** 1948, pp. 602–631.
5. Bode, Hendrik W., *Network Analysis and Feedback Amplifier Design*, New York, D. Van Nostrand, 1945.
6. Thomas, D. E., B.S.T.J., **26,** July, 1947, pp. 870–899. Reprinted as Bell System Monograph B-1511; also Seven-Figure Tables of Phase of a Semi-Infinite Unit Attenuation Slope, Bell System Monograph 2550.
7. Van Vleck, J. H., *Radiation Laboratory Series*, New York, McGraw-Hill, 1948, Vol. **13,** Ch. 8.
8. Miller, Richard A., and Lopez, Adolfo, Note on the Velocity of Light, Jour. Opt. Soc. Am., **49,** 1959, p. 930.
9. Bennett, W. R., Jr., Hole Burning Effects in a He-Ne Optical Maser, Phys. Rev., **126,** No. 2, 1962, pp. 580–593.
10. Faust, W. L., and Thomas, D. E., to be published.
11. Wood, Robert W., *Physical Optics*, New York, MacMillan Co., 1959, pp. 487–89.
12. Thomas, D. E., Proc. I.R.E., **40,** 1952, pp. 1481–83.
13. Thomas, D. E., and Moll, J. L., Proc. I.R.E., **46,** 1958, pp. 1177–1184.

Tables III and IV — Tables of Phase of a Semi-Infinite Unit Attenuation Slope

f/f_0 or f_0/f	Table III $f < f_0$ B in Radians	Table IV $f > f_0$ B in Radians	1st Difference
.999 700	0.784 4618	0.786 3346	
710	4898	3065	.0⁴281
720	5180	2783	282
730	5464	2500	283
740	5748	2216	284
			286
.999 750	0.784 6033	0.786 1930	
760	6320	1643	.0⁴287
770	6608	1355	288
780	6898	1066	289
790	7189	0775	291
			293
.999 800	0.784 7481	0.786 0482	
810	7775	0188	.0⁴294
820	8071	0.785 9893	295
830	8368	9595	298
840	8668	9296	299
			302
.999 850	0.784 8969	0.785 8994	
860	9273	8691	.0⁴303
870	9578	8385	306
880	9886	8077	308
890	0.785 0197	7766	311
			314
.999 900	0.785 0510 79	0.785 7452 48	
901	0542 33	7420 94	.0⁵3154
902	0573 91	7389 36	58
903	0605 51	7357 75	61
904	0637 15	7326 11	64
			67
.999 905	0.785 0668 83	0.785 7294 44	
906	0700 53	7262 73	.0⁵3171
907	0732 27	7230 99	74
908	0764 05	7199 22	77
909	0795 86	7167 41	81
			84
.999 910	0.785 0827 70	0.785 7135 57	
911	0859 58	7103 69	.0⁵3188
912	0891 50	7071 77	92
913	0923 45	7039 82	95
914	0955 44	7007 83	99
			3202
.999 915	0.785 0987 46	0.785 6975 81	
916	1019 52	6943 74	.0⁵3207
917	1051 62	6911 64	10
918	1083 76	6879 50	14
919	1115 94	6847 33	17
			22
.999 920	0.785 1148 16	0.785 6815 11	
921	1180 41	6782 85	.0⁵3226
922	1212 71	6750 56	29
923	1245 05	6718 22	34
924	1277 43	6685 84	38
			42
.999 925	0.785 1309 85	0.785 6653 42	
926	1342 31	6620 96	.0⁵3246
927	1374 82	6588 45	51
928	1407 37	6555 90	55
929	1439 96	6523 31	59
			64

f/f_0 or f_0/f	Table III $f < f_0$ B in Radians	Table IV $f > f_0$ B in Radians	1st Difference
.999 930	0.785 1472 60	0.785 6490 67	
931	1505 28	6457 98	.0^{5}3269
932	1538 01	6425 25	73
933	1570 79	6392 48	77
934	1603 62	6359 65	83
			87
.999 935	0.785 1636 49	0.785 6326 78	
936	1669 41	6293 86	.0^{5}3292
937	1702 38	6260 89	97
938	1735 40	6227 87	3303
939	1768 48	6194 79	08
			13
.999 940	0.785 1801 60	0.785 6161 67	
941	1834 78	6128 49	.0^{5}3318
942	1868 01	6095 26	23
943	1901 30	6061 97	29
944	1934 64	6028 63	34
			40
.999 945	0.785 1968 04	0.785 5995 23	
946	2001 50	5961 77	.0^{5}3346
947	2035 02	5928 25	52
948	2068 59	5894 68	57
949	2102 23	5861 04	64
			70
.999 950	0.785 2135 93	0.785 5827 34	
951	2169 69	5793 57	.0^{5}3377
952	2203 52	5759 75	82
953	2237 42	5725 85	90
954	2271 38	5691 89	96
			3403
.999 955	0.785 2305 41	0.785 5657 86	
956	2339 51	5623 75	.0^{5}3411
957	2373 69	5589 58	17
958	2407 94	5555 33	25
959	2442 26	5521 00	33
			40
.999 960	0.785 2476 67	0.785 5486 60	
961	2511 15	5452 12	.0^{5}3448
962	2545 71	5417 56	56
963	2580 36	5382 91	65
964	2615 09	5348 18	73
			82
.999 965	0.785 2649 91	0.785 5313 36	
966	2684 83	5278 44	.0^{5}3492
967	2719 83	5243 44	3500
968	2754 93	5208 33	11
969	2790 14	5173 13	20
			30
.999 970	0.785 2825 44	0.785 5137 83	
971	2860 85	5102 42	.0^{5}3541
972	2896 37	5066 90	52
973	2932 01	5031 26	64
974	2967 76	4995 51	75
			88
.999 975	0.785 3003 63	0.785 4959 63	
976	3039 63	4923 63	.0^{5}3600
977	3075 77	4887 50	13
978	3112 04	4851 23	27
979	3148 46	4814 81	42
			57

f/f_0 or f_0/f	Table III $f < f_0$ B in Radians	Table IV $f > f_0$ B in Radians	1st Difference
.999 9800	0.785 3185 03	0.785 4778 24	
01	3188 69	4774 57	.0^{5}0367
02	3192 36	4770 91	67
03	3196 03	4767 24	67
04	3199 70	4763 57	67
			67
.999 9805	0.785 3203 37	0.785 4759 90	
06	3207 05	4756 22	.0^{5}0367
07	3210 72	4752 55	68
08	3214 40	4748 87	68
09	3218 08	4745 19	68
			68
.999 9810	0.785 3221 76	0.785 4741 51	
11	3225 44	4737 83	.0^{5}0368
12	3229 12	4734 15	68
13	3232 81	4730 46	69
14	3236 50	4726 77	69
			69
.999 9815	0.785 3240 18	0.785 4723 08	
16	3243 87	4719 39	.0^{5}0369
17	3247 57	4715 70	69
18	3251 26	4712 01	69
19	3254 96	4708 31	70
			70
.999 9820	0.785 3258 65	0.785 4704 61	
21	3262 35	4700 92	.0^{5}0370
22	3266 05	4697 21	70
23	3269 76	4693 51	70
24	3273 46	4689 81	70
			71
.999 9825	0.785 3277 17	0.785 4686 10	
26	3280 88	4682 39	.0^{5}0371
27	3284 59	4678 68	71
28	3288 30	4674 97	71
29	3292 01	4671 26	71
			72
.999 9830	0.785 3295 73	0.785 4667 54	
31	3299 44	4663 82	.0^{5}0372
32	3303 16	4660 11	72
33	3306 88	4656 38	72
34	3310 61	4652 66	72
			73
.999 9835	0.785 3314 33	0.785 4648 94	
36	3318 06	4645 21	.0^{5}0373
37	3321 79	4641 48	73
38	3325 52	4637 75	73
39	3329 25	4634 02	73
			73
.999 9840	0.785 3332 99	0.785 4630 28	
41	3336 72	4626 54	.0^{5}0374
42	3340 46	4622 81	74
43	3344 20	4619 07	74
44	3347 95	4615 32	74
			74
.999 9845	0.785 3351 69	0.785 4611 58	
46	3355 44	4607 83	.0^{5}0375
47	3359 19	4604 08	75
48	3362 94	4600 33	75
49	3366 69	4596 58	75
			76

f/f_0 or f_0/f	Table III $f < f_0$ B in Radians	Table IV $f > f_0$ B in Radians	1st Difference
.999 9850	0.785 3370 45	0.785 4592 82	
51	3374 20	4589 06	.0^{5}0376
52	3377 96	4585 31	76
53	3381 72	4581 54	76
54	3385 49	4577 78	76
			77
.999 9855	0.785 3389 25	0.785 4574 01	
56	3393 02	4570 25	.0^{5}0377
57	3396 79	4566 48	77
58	3400 57	4562 70	77
59	3404 34	4558 93	77
			78
.999 9860	0.785 3408 12	0.785 4555 15	
61	3411 90	4551 37	.0^{5}0378
62	3415 68	4547 59	78
63	3419 46	4543 81	78
64	3423 25	4540 02	79
			79
.999 9865	0.785 3427 04	0.785 4536 23	
66	3430 83	4532 44	.0^{5}0379
67	3434 62	4528 65	79
68	3438 42	4524 85	80
69	3442 22	4521 05	80
			80
.999 9870	0.785 3446 02	0.785 4517 25	
71	3449 82	4513 45	.0^{5}0380
72	3453 62	4509 64	81
73	3457 43	4505 84	81
74	3461 24	4502 02	81
			81
.999 9875	0.785 3465 06	0.785 4498 21	
76	3468 87	4494 40	.0^{5}0382
77	3472 69	4490 58	82
78	3476 51	4486 76	82
79	3480 33	4482 93	82
			83
.999 9880	0.785 3484 16	0.785 4479 11	
81	3487 99	4475 28	.0^{5}0383
82	3491 82	4471 45	83
83	3495 65	4467 61	83
84	3499 49	4463 78	84
			84
.999 9885	0.785 3503 33	0.785 4459 94	
86	3507 17	4456 10	.0^{5}0384
87	3511 02	4452 25	84
88	3514 87	4448 40	85
89	3518 72	4444 55	85
			85
.999 9890	0.785 3522 57	0.785 4440 70	
91	3526 43	4436 84	.0^{5}0386
92	3530 29	4432 98	86
93	3534 15	4429 12	86
94	3538 01	4425 25	87
			87
.999 9895	0.785 3541 88	0.785 4421 39	
96	3545 75	4417 51	.0^{5}0387
97	3549 63	4413 64	87
98	3553 50	4409 76	88
99	3557 39	4405 88	88
			88

f/f_0 or f_0/f	Table III $f < f_0$ B in Radians	Table IV $f > f_0$ B in Radians	1st Difference
.999 9900	0.785 3561 27	0.785 4402 00	
01	3565 16	4398 11	.0^{5}0388
02	3569 05	4394 22	89
03	3572 94	4390 33	89
04	3576 84	4386 43	89
			90
.999 9905	0.785 3580 74	0.785 4382 53	
06	3584 64	4378 63	.0^{5}0390
07	3588 55	4374 72	91
08	3592 46	4370 81	91
09	3596 37	4366 90	91
			92
.999 9910	0.785 3600 29	0.785 4362 98	
11	3604 21	4359 06	.0^{5}0392
12	3608 13	4355 14	92
13	3612 06	4351 21	93
14	3615 99	4347 28	93
			94
.999 9915	0.785 3619 93	0.785 4343 34	
16	3623 87	4339 40	.0^{5}0394
17	3627 81	4335 46	94
18	3631 76	4331 51	95
19	3635 71	4327 56	95
			95
.999 9920	0.785 3639 66	0.785 4323 61	
21	3643 62	4319 65	.0^{5}0396
22	3647 58	4315 69	96
23	3651 55	4311 72	97
24	3655 52	4307 75	97
			97
.999 9925	0.785 3659 49	0.785 4303 77	
26	3663 47	4299 80	.0^{5}0398
27	3667 46	4295 81	98
28	3671 44	4291 82	99
29	3675 44	4287 83	99
			0400
.999 9930	0.785 3679 43	0.785 4283 84	
31	3683 43	4279 83	.0^{5}0400
32	3687 44	4275 83	01
33	3691 45	4271 82	01
34	3695 46	4267 80	02
			02
.999 9935	0.785 3699 48	0.785 4263 78	
36	3703 51	4259 76	.0^{5}0402
37	3707 54	4255 73	03
38	3711 57	4251 69	03
39	3715 61	4247 65	04
			05
.999 9940	0.785 3719 66	0.785 4243 61	
41	3723 71	4239 56	.0^{5}0405
52	3727 77	4235 50	06
43	3731 83	4231 44	06
44	3735 89	4227 37	07
			07
.999 9945	0.785 3739 97	0.785 4223 30	
46	3744 05	4219 22	.0^{5}0408
47	3748 13	4215 14	08
48	3752 22	4211 05	09
49	3756 32	4206 95	10
			10

f/f_0 or f_0/f	Table III $f < f_0$ B in Radians	Table IV $f > f_0$ B in Radians	1st Difference
.999 9950	0.785 3760 42	0.785 4202 85	
51	3764 53	4198 74	.0⁵0411
52	3768 65	4194 62	12
53	3772 77	4190 50	12
54	3776 90	4186 37	13
			14
.999 9955	0.785 3781 03	0.785 4182 24	
56	3785 18	4178 09	.0⁵0414
57	3789 33	4173 94	15
58	3793 48	4169 78	16
59	3797 65	4165 62	17
			17
.999 9960	0.785 3801 82	0.785 4161 45	
61	3806 00	4157 26	.0⁵0418
62	3810 19	4153 08	19
63	3814 39	4148 88	20
64	3818 60	4144 67	21
			22
.999 9965	0.785 3822 81	0.785 4140 46	
66	3827 04	4136 23	.0⁵0422
67	3831 27	4132 00	23
68	3835 51	4127 76	24
69	3839 76	4123 50	25
			26
.999 9970	0.785 3844 03	0.785 4119 24	
71	3848 30	4114 97	.0⁵0427
72	3852 59	4110 68	28
73	3856 88	4106 39	29
74	3861 19	4102 08	31
			32
.999 9975	0.785 3865 51	0.785 4097 76	
76	3869 85	4093 42	.0⁵0433
77	3874 19	4089 08	35
78	3878 55	4084 72	36
79	3882 93	4080 34	37
			39
.999 9980	0.785 3887 32	0.785 4075 95	
81	3891 72	4071 55	.0⁵0441
82	3896 14	4067 12	42
83	3900 58	4062 68	44
84	3905 04	4058 23	46
			48
.999 9985	0.785 3909 52	0.785 4053 75	
86	3914 02	4049 25	.0⁵0450
87	3918 54	4044 72	52
88	3923 09	4040 18	55
89	3927 67	4035 60	57
			60
.999 9990	0.785 3932 27	0.785 4031 00	
91	3936 90	4026 37	.0⁵0463
92	3941 57	4021 69	67
93	3946 28	4016 98	71
94	3951 04	4012 23	76
			81
.999 9995	0.785 3955 85	0.785 4007 42	
96	3960 72	4002 55	.0⁵0487
97	3965 68	3997 59	96
			0506
.999 99980	0.785 3970 74	0.785 3992 53	
985	3973 32	3989 94	.0⁵0259
990	3975 96	3987 30	64
995	3978 68	3984 58	72
			95
1.000 00000	0.785 3981 63	0.785 3981 63	

TABLE V — Φ IN RADIANS FOR LINE SEGMENT, A, OF 1 NEPER; $f_{12} = 10^6$ CPS

Δf_{12}	$\Delta f = 2$	$\Delta f = 4$	$\Delta f = 6$	$\Delta f = 10$	$\Delta f = 20$	$\Delta f = 40$
0	4.936	4.716	4.587	4.424	4.204	3.983
1	4.716	4.674	4.569	4.418	4.202	3.983
2	4.412	4.496	4.510	4.398	4.197	3.981
3	4.275	4.296	4.366	4.363	4.189	3.979
4	4.180	4.192	4.214	4.307	4.177	3.977
5	4.108	4.115	4.128	4.204	4.162	3.973
6	4.050	4.054	4.062	4.097	4.142	3.968
7	4.000	4.003	4.007	4.032	4.116	3.963
8	3.957	3.960	3.964	3.980	4.086	3.957
9	3.920	3.922	3.925	3.937	4.046	3.950
10	3.886	3.888	3.890	3.900	3.983	3.941
11	3.856	3.857	3.859	3.867	3.919	3.932
12	3.828	3.829	3.831	3.837	3.876	3.922
13	3.802	3.803	3.805	3.810	3.841	3.910
14	3.778	3.779	3.781	3.785	3.811	3.897
15	3.756	3.757	3.758	3.762	3.784	3.882
16	3.736	3.736	3.738	3.741	3.760	3.866
17	3.716	3.717	3.718	3.721	3.737	3.847
18	3.698	3.699	3.700	3.703	3.716	3.826
19	3.682	3.682	3.682	3.685	3.697	3.800
20	3.665	3.666	3.666	3.668	3.679	3.762
21	3.650	3.650	3.650	3.652	3.662	3.725
22	3.634	3.635	3.635	3.637	3.646	3.698
23	3.620	3.620	3.621	3.623	3.631	3.676
24	3.606	3.607	3.607	3.609	3.616	3.656
25	3.594	3.594	3.594	3.596	3.603	3.638
26	3.582	3.582	3.582	3.583	3.590	3.621
27	3.570	3.570	3.570	3.571	3.577	3.605
28	3.558	3.558	3.558	3.559	3.565	3.590
29	3.546	3.547	3.547	3.548	3.553	3.576
30	3.536	3.536	3.536	3.537	3.542	3.563
31	3.525	3.526	3.526	3.527	3.531	3.551
32	3.516	3.515	3.516	3.516	3.520	3.539
33	3.506	3.506	3.506	3.507	3.510	3.528
34	3.496	3.496	3.496	3.497	3.501	3.517
35	3.487	3.487	3.487	3.488	3.491	3.506
36	3.478	3.478	3.478	3.479	3.482	3.496
37	3.469	3.469	3.469	3.470	3.473	3.486
38	3.460	3.460	3.461	3.461	3.464	3.477
39	3.452	3.452	3.452	3.453	3.456	3.467
40	3.444	3.444	3.444	3.445	3.448	3.459
41	3.436	3.436	3.436	3.437	3.440	3.450
42	3.429	3.429	3.429	3.429	3.432	3.442
43	3.421	3.422	3.421	3.422	3.424	3.433
44	3.414	3.414	3.414	3.414	3.417	3.426
45	3.407	3.407	3.407	3.407	3.409	3.418
46	3.400	3.400	3.400	3.400	3.402	3.410
47	3.393	3.393	3.393	3.394	3.395	3.403
48	3.386	3.386	3.386	3.387	3.389	3.396
49	3.380	3.380	3.380	3.380	3.382	3.389

TABLE V — *Continued*

Δf_{12}	$\Delta f \leqq 20$	$\Delta f = 40$	Δf_{12}	$\Delta f \leqq 20$	$\Delta f = 40$
50	3.374	3.382	90	3.186	3.189
51	3.367	3.375	91	3.183	3.185
52	3.361	3.369	92	3.179	3.181
53	3.355	3.362	93	3.176	3.178
54	3.349	3.356	94	3.172	3.174
55	3.343	3.350	95	3.169	3.171
56	3.337	3.344	96	3.166	3.168
57	3.332	3.338	97	3.162	3.164
58	3.326	3.332	98	3.159	3.161
59	3.321	3.327	99	3.156	3.158
60	3.315	3.321	100	3.152	3.155
61	3.310	3.316	101	3.149	3.151
62	3.305	3.310	102	3.146	3.148
63	3.300	3.305	103	3.143	3.145
64	3.295	3.300	104	3.140	3.142
65	3.290	3.295	105	3.137	3.139
66	3.285	3.290	106	3.134	3.136
67	3.280	3.285	107	3.131	3.133
68	3.275	3.280	108	3.128	3.130
69	3.271	3.275	109	3.125	3.127
70	3.266	3.270	110	3.122	3.124
71	3.262	3.266	111	3.119	3.121
72	3.257	3.261	112	3.116	3.118
73	3.253	3.257	113	3.114	3.115
74	3.248	3.252	114	3.111	3.112
75	3.244	3.248	115	3.108	3.110
76	3.240	3.243	116	3.105	3.107
77	3.236	3.239	117	3.103	3.104
78	3.232	3.235	118	3.100	3.101
79	3.228	3.231	119	3.097	3.099
80	3.224	3.227	120	3.094	3.096
81	3.220	3.223	121	3.092	3.093
82	3.216	3.219	122	3.089	3.091
83	3.212	3.215	123	3.087	3.088
84	3.208	3.211	124	3.084	3.085
85	3.204	3.207	125	3.081	3.083
86	3.201	3.203	126	3.079	3.080
87	3.197	3.200	127	3.076	3.078
88	3.193	3.196	128	3.074	3.075
89	3.190	3.192	129	3.071	3.073

Δf_{12}	$\Delta f \leqq 40$	Δf_{12}	$f\Delta \leqq 40$	Δf_{12}	$\Delta f \leqq 40$	Δf_{12}	$\Delta f \leqq 40$
130	3.069	140	3.045	150	3.023	160	3.003
131	3.066	141	3.043	151	3.021	161	3.001
132	3.064	142	3.041	152	3.019	162	2.999
133	3.062	143	3.039	153	3.017	163	2.997
134	3.059	144	3.036	154	3.015	164	2.995
135	3.057	145	3.034	155	3.013	165	2.993
136	3.055	146	3.032	156	3.011	166	2.991
137	3.052	147	3.030	157	3.009	167	2.989
138	3.050	148	3.028	158	3.007	168	2.987
139	3.048	149	3.026	159	3.005	169	2.985

TABLE V — *Continued*

Δf_{12}	$\Delta f \leqq 40$	Δf_{12}	$\Delta f \leqq 40$	Δf_{12}	$\Delta f \leqq 40$	Δf_{12}	$\Delta f \leqq 40$
170	2.984	220	2.901	270	2.836	500	2.640
171	2.982	221	2.900	271	2.835	510	2.634
172	2.980	222	2.899	272	2.834	520	2.628
173	2.978	223	2.897	273	2.833	530	2.622
174	2.976	224	2.896	274	2.832	540	2.616
175	2.974	225	2.894	275	2.831	550	2.610
176	2.972	226	2.893	276	2.829	560	2.604
177	2.971	227	2.891	277	2.828	570	2.598
178	2.969	228	2.890	278	2.827	580	2.593
179	2.967	229	2.889	279	2.826	590	2.587
180	2.965	230	2.887	280	2.825	600	2.582
181	2.964	231	2.886	281	2.824	610	2.577
182	2.962	232	2.885	282	2.822	620	2.572
183	2.960	233	2.883	283	2.821	630	2.567
184	2.958	234	2.882	284	2.820	640	2.562
185	2.957	235	2.880	285	2.819	650	2.557
186	2.955	236	2.879	286	2.818	660	2.552
187	2.953	237	2.878	287	2.817	670	2.547
188	2.951	238	2.876	288	2.816	680	2.542
189	2.950	239	2.875	289	2.815	690	2.538
190	2.948	240	2.874	290	2.813	700	2.533
191	2.946	241	2.872	291	2.812	710	2.528
192	2.945	242	2.871	292	2.811	720	2.524
193	2.943	243	2.870	293	2.810	730	2.520
194	2.941	244	2.868	294	2.809	740	2.516
195	2.940	245	2.867	295	2.808	750	2.511
196	2.938	246	2.866	297	2.807	760	2.507
197	2.937	247	2.865	297	2.806	770	2.503
198	2.935	248	2.863	298	2.805	780	2.499
199	2.933	249	2.862	299	2.804	790	2.494
200	2.932	250	2.861	300	2.803	800	2.490
201	2.930	251	2.859	310	2.792	810	2.487
202	2.929	252	2.858	320	2.782	820	2.483
203	2.927	253	2.857	330	2.772	830	2.479
204	2.925	254	2.856	340	2.763	840	2.475
205	2.924	255	2.854	350	2.754	850	2.471
206	2.922	256	2.853	360	2.745	860	2.467
207	2.921	257	2.852	370	2.736	870	2.464
208	2.919	258	2.851	380	2.727	880	2.460
209	2.918	259	2.849	390	2.719	890	2.457
210	2.916	260	2.848	400	2.711	900	2.453
211	2.915	261	2.847	410	2.703	910	2.449
212	2.913	262	2.846	420	2.696	920	2.446
213	2.912	263	2.845	430	2.688	930	2.443
214	2.910	264	2.843	440	2.681	940	2.439
215	2.909	265	2.842	450	2.674	950	2.436
216	2.907	266	2.841	460	2.667	960	2.432
217	2.906	267	2.840	470	2.660	970	2.429
218	2.904	268	2.839	480	2.653	980	2.426
219	2.903	269	2.837	490	2.647	990	2.423

1000	2.419

TABLE VI — $\Psi_{500+n-(f+1)}$ IN RADIANS PER NEPER

$500+n-(f+1)$	Ψ	$500+n-(f+1)$	Ψ	$500+n-(f+1)$	Ψ
0	−.00128	100	−.00159	200	−.00212
2	−.00128	102	−.00160	202	−.00214
4	−.00129	104	−.00161	204	−.00216
6	−.00129	106	−.00162	206	−.00218
8	−.00130	108	−.00163	208	−.00219
10	−.00130	110	−.00164	210	−.00220
12	−.00131	112	−.00164	212	−.00222
14	−.00131	114	−.00165	214	−.00224
16	−.00132	116	−.00166	216	−.00225
18	−.00132	118	−.00167	218	−.00227
20	−.00133	120	−.00168	220	−.00229
22	−.00133	122	−.00169	222	−.00230
24	−.00134	124	−.00170	224	−.00232
26	−.00135	126	−.00171	226	−.00234
28	−.00135	128	−.00171	228	−.00235
30	−.00136	130	−.00172	230	−.00237
32	−.00136	132	−.00173	232	−.00239
34	−.00137	134	−.00174	234	−.00240
36	−.00137	136	−.00175	236	−.00242
38	−.00138	138	−.00176	238	−.00244
40	−.00138	140	−.00177	240	−.00246
42	−.00139	142	−.00178	242	−.00248
44	−.00139	144	−.00179	244	−.00250
46	−.00140	146	−.00180	246	−.00252
48	−.00141	148	−.00181	248	−.00254
50	−.00142	150	−.00182	250	−.00256
52	−.00143	152	−.00183	252	−.00258
54	−.00143	154	−.00184	254	−.00260
56	−.00144	156	−.00185	256	−.00262
58	−.00144	158	−.00186	258	−.00264
60	−.00145	160	−.00187	260	−.00266
62	−.00146	162	−.00188	262	−.00269
64	−.00146	164	−.00189	264	−.00271
66	−.00147	166	−.00190	266	−.00273
68	−.00148	168	−.00192	268	−.00275
70	−.00149	170	−.00193	270	−.00277
72	−.00150	172	−.00195	272	−.00280
74	−.00150	174	−.00196	274	−.00283
76	−.00151	176	−.00197	276	−.00286
78	−.00151	178	−.00198	278	−.00288
80	−.00152	180	−.00200	280	−.00291
82	−.00153	182	−.00201	282	−.00294
84	−.00154	184	−.00202	284	−.00297
86	−.00154	186	−.00203	286	−.00300
88	−.00155	188	−.00205	288	−.00302
90	−.00156	190	−.00206	290	−.00305
92	−.00156	192	−.00207	292	−.00308
94	−.00157	194	−.00208	294	−.00311
96	−.00158	196	−.00209	296	−.00314
98	−.00159	198	−.00210	298	−.00317

TABLE VI — *Continued*

$500 + n - (f+1)$	Ψ	$500 + n - (f+1)$	Ψ	$500 + n - (f+1)$	Ψ
300	−.00320	400	−.00644	500	+.52454
302	−.00323	402	−.00657	502	+.23165
304	−.00327	404	−.00671	504	+.13096
306	−.00330	406	−.00685	506	+.09219
308	−.00334	408	−.00700	508	+.07134
310	−.00337	410	−.00717	510	+.05189
312	−.00341	412	−.00732	512	+.04916
314	−.00344	414	−.00748	514	+.04256
316	−.00348	416	−.00767	516	+.03753
318	−.00352	418	−.00785	518	+.03356
320	−.00356	420	−.00805	520	+.03036
322	−.00360	422	−.00827	522	+.02770
324	−.00365	424	−.00848	524	+.02549
326	−.00368	426	−.00872	526	+.02359
328	−.00372	428	−.00895	528	+.02197
330	−.00376	430	−.00923	530	+.02054
332	−.00381	432	−.00950	532	+.01930
334	−.00386	434	−.00979	534	+.01819
336	−.00391	436	−.01010	536	+.01721
338	−.00396	438	−.01043	538	+.01632
340	−.00401	440	−.01079	540	+.01553
342	−.00406	442	−.01116	542	+.01480
344	−.00411	444	−.01158	544	+.01415
346	−.00416	446	−.01201	546	+.01354
348	−.00422	448	−.01248	548	+.01299
350	−.00428	450	−.01299	550	+.01248
352	−.00433	452	−.01354	552	+.01201
354	−.00439	454	−.01415	554	+.01158
356	−.00445	456	−.01480	556	+.01116
358	−.00452	458	−.01553	558	+.01079
360	−.00458	460	−.01632	560	+.01043
362	−.00464	462	−.01721	562	+.01010
364	−.00471	464	−.01819	564	+.00979
366	−.00478	466	−.01930	566	+.00950
368	−.00486	468	−.02054	568	+.00923
370	−.00494	470	−.02197	570	+.00895
372	−.00502	472	−.02359	572	+.00872
374	−.00510	474	−.02549	574	+.00848
376	−.00518	476	−.02770	576	+.00827
378	−.00527	478	−.03036	578	+.00805
380	−.00536	480	−.03356	580	+.00785
382	−.00546	482	−.03753	582	+.00767
384	−.00555	484	−.04256	584	+.00748
386	−.00564	486	−.04916	586	+.00732
388	−.00573	488	−.05819	588	+.00717
390	−.00583	490	−.07134	590	+.00700
392	−.00595	492	−.09219	592	+.00685
394	−.00607	494	−.13096	594	+.00671
396	−.00619	496	−.23165	596	+.00657
398	−.00632	498	−.52454	598	+.00644

TABLE VI — *Continued*

$500 + n - (f+1)$	Ψ	$500 + n - (f+1)$	Ψ	$500 + n - (f+1)$	Ψ
600	+.00632	700	+.00317	800	+.00210
602	+.00619	702	+.00314	802	+.00209
604	+.00607	704	+.00311	804	+.00208
606	+.00595	706	+.00308	806	+.00207
608	+.00583	708	+.00305	808	+.00206
610	+.00573	710	+.00302	810	+.00205
612	+.00564	712	+.00300	812	+.00203
614	+.00555	714	+.00297	814	+.00202
616	+.00546	716	+.00294	816	+.00201
618	+.00536	718	+.00291	818	+.00200
620	+.00527	720	+.00288	820	+.00198
622	+.00518	722	+.00286	822	+.00197
624	+.00510	724	+.00283	824	+.00196
626	+.00502	726	+.00280	826	+.00195
628	+.00494	728	+.00277	828	+.00193
630	+.00486	730	+.00275	830	+.00192
632	+.00478	732	+.00273	832	+.00190
634	+.00471	734	+.00271	834	+.00189
636	+.00464	736	+.00269	836	+.00188
638	+.00458	738	+.00266	838	+.00187
640	+.00452	740	+.00264	840	+.00186
642	+.00445	742	+.00262	842	+.00185
644	+.00439	744	+.00260	844	+.00184
646	+.00433	746	+.00258	846	+.00183
648	+.00428	748	+.00256	848	+.00182
650	+.00422	750	+.00254	850	+.00181
652	+.00416	752	+.00252	852	+.00180
654	+.00411	754	+.00250	854	+.00179
656	+.00406	756	+.00248	856	+.00178
658	+.00401	758	+.00246	858	+.00177
660	+.00396	760	+.00244	860	+.00176
662	+.00391	762	+.00242	862	+.00175
664	+.00386	764	+.00240	864	+.00174
666	+.00381	766	+.00239	866	+.00173
668	+.00376	768	+.00237	868	+.00172
670	+.00372	770	+.00235	870	+.00171
672	+.00368	772	+.00234	872	+.00171
674	+.00365	774	+.00232	874	+.00170
676	+.00360	776	+.00230	876	+.00169
678	+.00356	778	+.00229	878	+.00168
680	+.00352	780	+.00227	880	+.00167
682	+.00348	782	+.00225	882	+.00166
684	+.00344	784	+.00224	884	+.00165
686	+.00341	786	+.00222	886	+.00164
688	+.00337	788	+.00220	888	+.00164
690	+.00334	790	+.00219	890	+.00163
692	+.00330	792	+.00218	892	+.00162
694	+.00327	794	+.00216	894	+.00161
696	+.00323	796	+.00214	896	+.00160
698	+.00320	798	+.00212	898	+.00159

TABLE VI — *Continued*

$500 + n - (f+1)$	Ψ	$500 + n - (f+1)$	Ψ	$500 + n - (f+1)$	Ψ
900	+.00159	940	+.00144	980	+.00132
902	+.00158	942	+.00144	982	+.00132
904	+.00157	944	+.00143	984	+.00131
906	+.00156	946	+.00143	986	+.00131
908	+.00156	948	+.00142	988	+.00130
910	+.00155	950	+.00141	990	+.00130
912	+.00154	952	+.00140	992	+.00129
914	+.00154	954	+.00139	994	+.00129
916	+.00153	956	+.00139	996	+.00128
918	+.00152	958	+.00138	998	+.00128
920	+.00151	960	+.00138	1000	+.00127
922	+.00151	962	+.00137		
924	+.00150	964	+.00137		
926	+.00150	966	+.00136		
928	+.00149	968	+.00136		
930	+.00148	970	+.00135		
932	+.00147	972	+.00135		
934	+.00146	974	+.00134		
936	+.00146	976	+.00133		
938	+.00145	978	+.00133		

TABLE VII — LINE SEGMENT PHASE SUMMATION — TRUNCATED GAUSSIAN SECTION

f	Line $f_{12} = 3$ ab Δf_{12}	Φ_{ab}	Line $f_{12} = 9$ bc Δ_{12}	Φ_{bc}	Line $f_{12} = 71$ $c'd$ Δf_{12}	$\Phi_{c'd}$	Line $f_{12} = 77$ de Δf_{12}	Φ_{de}	$\theta(f)$ radians
0	3	4.366	9	3.925	71	3.262	77	3.236	0.1901
2	1	4.569	7	4.007	69	3.271	75	3.244	0.2185
4	1	4.569	5	4.128	67	3.280	73	3.253	0.2294
6	3	4.366	3	4.366	65	3.290	71	3.262	0.2311
8	5	4.128	1	4.569	63	3.300	69	3.271	0.2254
10	7	4.007	1	4.569	61	3.310	67	3.280	0.2105
12	9	3.925	3	4.366	59	3.321	65	3.290	0.1781
14	11	3.859	5	4.128	57	3.332	63	3.300	0.1433
16	13	3.805	7	4.007	55	3.343	61	3.310	0.1229
18	15	3.758	9	3.925	53	3.355	59	3.321	0.1067
20	17	3.718	11	3.859	51	3.367	57	3.332	0.0931
22	19	3.682	13	3.805	49	3.380	55	3.343	0.0810
24	21	3.650	15	3.758	47	3.393	53	3.355	0.0700
26	23	3.621	17	3.718	45	3.407	51	3.367	0.0599
28	25	3.594	19	3.682	43	3.421	49	3.380	0.0504
30	27	3.570	21	3.650	41	3.436	47	3.393	0.0414
32	29	3.547	23	3.621	39	3.452	45	3.407	0.0328
34	31	3.526	25	3.594	37	3.469	43	3.421	0.0244
36	33	3.506	27	3.570	35	3.487	41	3.436	0.0162
38	35	3.487	29	3.547	33	3.506	39	3.452	0.0081
40	37	3.469	31	3.526	31	3.526	37	3.469	0.0000

$\theta(f) = A_n$ (Constant at 0.106 nepers)$(\Phi_{ab} + \Phi_{bc} - \Phi_{c'd} - \Phi_{de})$.